REVIEWS IN ADVANCE

Oblique, High-Angle, Listric-Reverse Faulting and Associated Development of Strain: The Wenchuan Earthquake of May 12, 2008, Sichuan, China

Pei-Zhen Zhang,[1] Xue-ze Wen,[2] Zheng-Kang Shen,[1] and Jiu-hui Chen[1]

[1]State Key Laboratory of Earthquake Dynamics, Institute of Geology, China Earthquake Administration, Beijing 100029, China; email: peizhen@ies.ac.cn, zshen@ies.ac.cn, chenjh@ies.ac.cn

[2]Sichuan Seismological Bureau, Chengdu 610041, China; email: xzwen@eqsc.gov.cn

Annu. Rev. Earth Planet. Sci. 2010. 38:351–80

The *Annual Review of Earth and Planetary Sciences* is online at earth.annualreviews.org

This article's doi:
10.1146/annurev-earth-040809-152602

0084-6597/10/0530-0351$20.00

Key Words

cascade earthquake rupture, stress accumulation and release, eastern Tibet, Longmen Shan fault, triggered slip

Abstract

The 2008 Wenchuan earthquake occurred on imbricate, oblique, steeply dipping, slowly slipping, listric-reverse faults. Measurements of coseismic slip, the distribution of aftershocks, and fault-plane solution of the mainshock all confirm this style of deformation and indicate cascading earthquake rupture of multiple segments, each with coseismic slip occurring in the shallow crust above a depth range of 10 to 12 km. Interactions among three geological units—eastern Tibet, the Longmen Shan, and the Sichuan basin—caused slow strain accumulation in the Longmen Shan so that measurable preearthquake slip was minor. Coseismic deformation, however, took place mostly within the interseismically locked Longmen Shan fault zone. The earthquake may have initiated from slip on a fault plane dipping 30–40° northwest in a depth range from 15 to 20 km and triggered oblique slip on the high-angle faults at depths shallower than 15 km to form the great Wenchuan earthquake.

INTRODUCTION

On May 12, 2008, a devastating earthquake struck densely populated Sichuan Province, China (31.0°N, 103.4°E) (CENC 2008). The event is named the Wenchuan earthquake as its epicenter is located in the administrative region of Wenchuan County. More than 80,000 people were killed, more than 370,000 people were injured, and economic losses were estimated at approximately 800 billion RMB (nearly $100 billion USD) (CENC 2008). The earthquake generated numerous landslides that destroyed lifelines, annihilated villages that clung to the steep slopes, and posed significant difficulties for rescue efforts. Both the surface-wave magnitude (M_s 8.0) reported by the China Earthquake Networks Center (CENC 2008) and the moment magnitude (M_w 7.9) given by different agencies and scientists (Ji 2008, Wang et al. 2008, Y. Zhang et al. 2008) attest to this event being a great earthquake. It is China's most disastrous event since the 1976 Tangshan earthquake, which killed more than 240,000 people.

Although the steep western margin of the Sichuan basin is known to be seismically active, few, if any, earth scientists anticipated an event of this magnitude to occur there. Two main observations contributed to this biased view. First, Global Positioning System (GPS) measurements (King et al. 1997, Chen et al. 2000, Zhang et al. 2004, Shen et al. 2005, Gan et al. 2007) and active faulting studies (Burchfiel et al. 1995, 2008; Densmore et al. 2007; Zhou et al. 2007) reveal very slow (<2–3 mm year^{-1}) slip rates across the Longmen Shan fault zone, indicative of relatively modest strain accumulation and therefore a slowly accumulating seismic hazard. Second, the most devastating, great reverse- or thrust-faulting historic earthquakes commonly rupture gently dipping thrust (not high-angle reverse) faults along which slip occurs rapidly (>50 mm year^{-1} at the oceanic subduction zones and >15 mm year^{-1} along the Himalaya collision zone). For example, the great earthquakes in Chile (1960), Alaska (1964), and Sumatra (2004) are all associated with geologically averaged slip rates that exceed 50 mm year^{-1} along gently dipping subduction-zone interfaces (Plafker 1969, Kanamori & Anderson 1975, Ammon et al. 2005, Lay et al. 2005, McCaffrey 2009). In addition, for the earthquakes in Kangra (1905), Bihar Nepal (1934), and Assam (1959), along the <15° dipping the Main Himalayan Thrust long-term slip rates are 15–20 mm year^{-1} (Lavé & Avouac 2000; Bilham et al. 2001; Kumar et al. 2001, 2006; Avouac 2003; Bollinger et al. 2004; Lavé et al. 2005). The 2008 Wenchuan earthquake, however, occurred on a high angle–dipping listric-reverse fault with a slip rate of less than 2–3 mm year^{-1} (Densmore et al. 2007, P.Z. Zhang et al. 2008, Zhou et al. 2007). To the best of our knowledge, the 2008 Wenchuan earthquake is the first with such a large magnitude to have occurred on a slowly slipping listric-reverse fault within continental interior during instrumentally recorded earthquake history.

TECTONIC FRAMEWORK OF THE LONGMEN SHAN FAULT ZONE

The Wenchuan earthquake ruptured several strands of the Longmen Shan fault zone, which lies along the middle segment of the Central Longitudinal Seismic Belt (CLSB) of China, along which more than 40 historical earthquakes of magnitude 7 and higher have occurred since the beginning of documented Chinese history (**Figure 1**). This belt separates the seismically active Tibetan

Figure 1

Regional tectonic map of the Longmen Shan region. (*a*) Topography, active faults, and earthquakes of the Tibetan Plateau. Earthquakes of magnitude higher than 6 are shown. White dashed polygon outlines approximate the area of the Central Longitudinal Seismic Belt (CLSB). (*b*) Active tectonic map of the Longmen Shan region [detail area from red-rectangle region in (*a*)]. GPS velocity vectors are relative to the South China block. Major active tectonic terrains are denoted by their names.

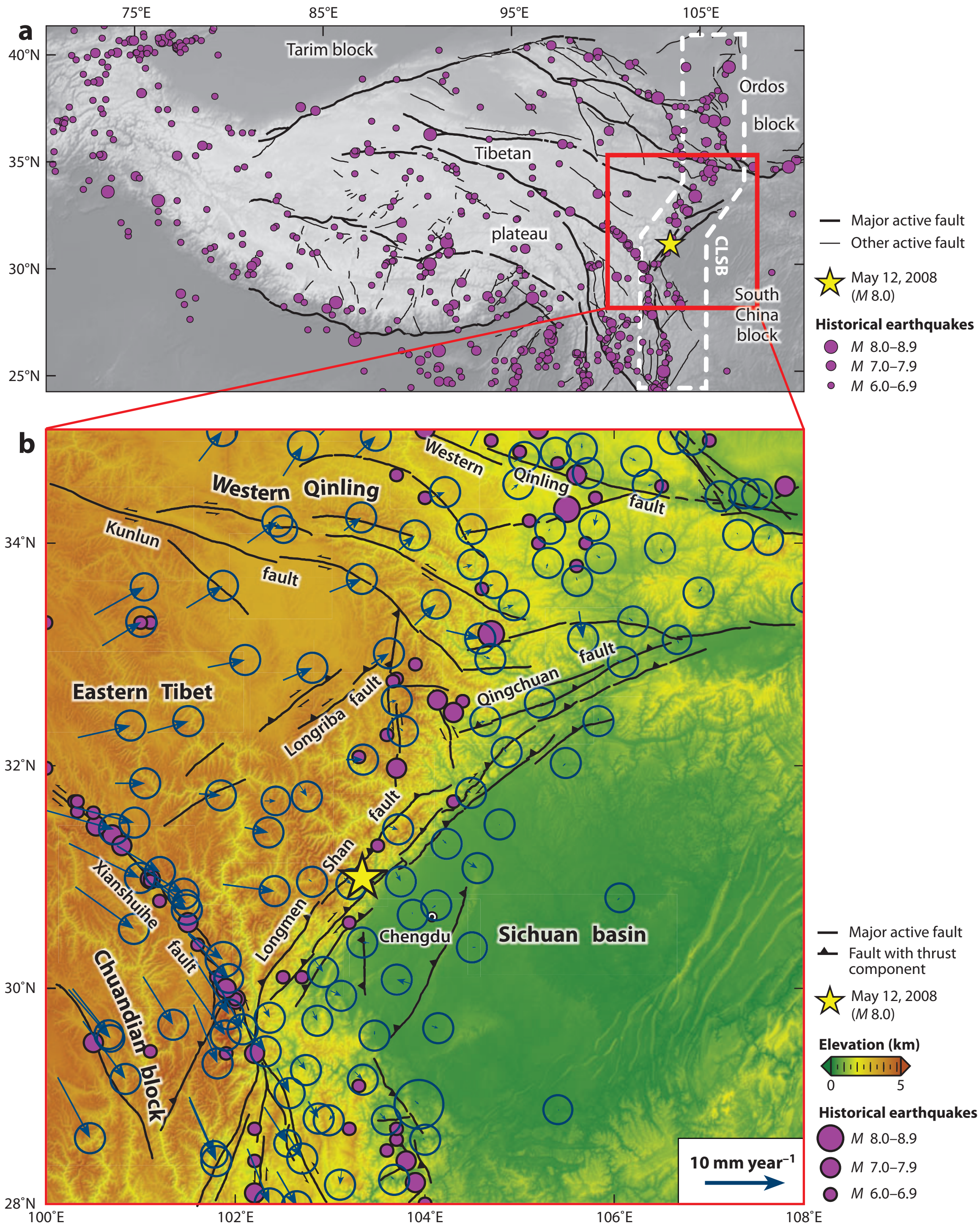
a
75°E
85°E
95°E
105°E
40°N
35°N
30°N
25°N
Tarim block
Tibetan
plateau
Ordos
block
CLSB
South
China
block
Major active fault
Other active fault
May 12, 2008
(M 8.0)
Historical earthquakes
M 8.0–8.9
M 7.0–7.9
M 6.0–6.9
b
34°N
32°N
30°N
28°N
100°E
102°E
104°E
106°E
108°E
Western Qinling
Western
Qinling
fault
Kunlun
fault
fault
Qingchuan
fault
Longriba
Eastern Tibet
fault
Shan
Longmen
Xianshuihe
fault
Chuandian block
Chengdu
Sichuan basin
10 mm year⁻¹
Major active fault
Fault with thrust component
May 12, 2008
(M 8.0)
Elevation (km)
0
5
Historical earthquakes
M 8.0–8.9
M 7.0–7.9
M 6.0–6.9

Plateau from the tectonically stable Ordos block, Sichuan basin, and South China block (Zhang et al. 2003, Zhang 2008). To its west, elevations reach more than 4000 m above sea level, the crust thickens to 50–60 km, and widespread active faulting attests to continued seismotectonic activity (Wang et al. 2007, Yao et al. 2008, L. Xu et al. 2007, Liu et al. 2009). East of this belt, however, the elevation of the Sichuan basin lies only ~600 m above sea level, the crustal thickness is only 40 to 45 km, and the absence of active faulting suggests relatively mild tectonic activity and a relatively low level of seismicity.

The active Longmen Shan fault zone marks a predominantly convergent boundary with a right-lateral strike-slip component. This fault system was reactivated during late Cenozoic time along a Mesozoic orogenic belt (Burchfiel et al. 1995, 2008; Kirby et al. 2002, 2008). To the west of the Longmen Shan, eastern Tibet (Songpan–Ganzi Terrain in geological terminology) actively deforms by both right-lateral shear parallel to and convergence perpendicular to the Longmen Shan fault (King et al. 1997, Chen et al. 2000, Zhang et al. 2004, Shen et al. 2005, Gan et al. 2007). Tectonic activity in the Sichuan basin, east of the Longmen Shan, has been mild during late Cenozoic time. Three principal, subparallel, active faults comprise the northeast-trending Longmen Shan fault zone (**Figure 1**). The Yingxiu-Beichuan fault, the major strand, coincides with the dramatic changes in the steepness of rugged topography (Kirby et al. 2008). The primary rupture of the 2008 Wenchuan earthquake occurred on this strand (X. Xu et al. 2008). The 2008 earthquake also ruptured a 73-km section of the Guanxian-Jiangyou fault, the eastern strand of the fault zone along the mountain front. The Wenchuan-Maoxian fault follows the Minjiang river valley approximately 30 kilometers northwest of the Yingxiu-Beichuan fault. The 2008 Wenchuan earthquake did not rupture this fault, but numerous landslides and debris flows occurred along it.

Average slip rates for the past ~10,000 years, however, have been estimated to be quite slow, approximately 0.3–0.6 mm year^{-1} for reverse faulting and ~1.0 mm year^{-1} for right-lateral strike-slip faulting on the Yingxiu-Beichuan fault, and 0.2 mm year^{-1} for reverse faulting on the Guanxian-Jiangyou fault (Densmore et al. 2007, Zhou et al. 2007). Ran et al. (2008) reports that the second terrace above the Minjiang riverbed at the town of Yingxiu has been displaced for 7.6 m including 2.4 m of coseismic offset during the Wenchuan earthquake. Numerous dates suggest that the terrace was abandoned between 3400 and 4000 years ago (Ran et al. 2008). Initiation of this terrace offset should postdate this abandonment age, and that age gives a minimum value of the slip rate. To remove the contribution of the recent earthquake cycle to the long-term slip rate, we subtracted the 2.4-m coseismic displacement of the 2008 Wenchuan earthquake from the total vertical offset of the terrace (Zhang et al. 1988, Li et al. 2009). Thus for the ~5.2-m, pre-2008 displacement of the terrace, the minimum long-term vertical slip rate would be 1.3 to 1.5 mm year^{-1}, which roughly coincides with previous estimates (Densmore et al. 2007, Zhou et al. 2007). Such geologically inferred average slip rates appropriate for several thousand years are consistent with GPS estimates of the shortening rate across the Longmen Shan range: <2–3 mm year^{-1} based on geodetic measurements made during the past two decades (King et al. 1997; Chen et al. 2000; P.Z. Zhang et al. 2004, 2008; Shen et al. 2005; Gan et al. 2007).

MAINSHOCK AND ITS RUPTURE PROCESS

The China Earthquake Networks Center reported an origin time (14:28:04 Beijing time) and a hypocenter location of the earthquake (31.0°N, 103.4°E, focal depth 14.5 km) (CENC 2008). The U.S. Geological Survey gave a similar result. A seismic array (the Western Sichuan Seismic Array, or WSSA) consisting of 297 broadband seismometers was deployed in the western Sichuan region at the end of 2006 (Liu et al. 2009). The mainshock took place within the northeastern quadrant of the array, allowing precise determination of hypocenter locations of the mainshock and aftershock sequence using local records.

Twenty WSSA seismic stations are located within a 75-km radius around the epicenter, and 12 of them recorded clear P-wave arrivals on their vertical components. Waveforms of these local stations show small direct waves that rapidly decrease in amplitude as they travel away from the epicenter. These small-amplitude waveforms cannot be seen in records of far-field stations, but they constrain crucial information about the precise hypocenter location of the mainshock. The improved results (Chen et al. 2009) show that initiation of the mainshock occurred at 14 h, 27 min, and 57.10 $\pm$ 0.03 s, and that the hypocenter is at 31.0032° $\pm$ 0.0024°N, 103.3694° $\pm$ 0.0025°E, and 18.7 $\pm$ 0.5 km.

Using 18 P-wave first motions and 27 P-wave waveforms from far-field seismic records, Wang et al. (2008) determined the focal mechanism of the mainshock: a seismic moment of 6.5×10^{20}, a strike of 229°, a dip of 32° toward the northwest, and a rake of 118° with predominantly unilaterally propagation of the rupture to the northeast. The fault-plane solution indicates mainly thrust slip with a right-lateral strike-slip component, corroborating geological observations of surface ruptures associated with this earthquake. Long-period P-waveform inversions performed by different parties show consistent results (Ji 2008, Nishimura & Yagi 2008, Y. Zhang et al. 2008, Global CMT Project).

Wang et al. (2008) used a finite fault model to determine the temporal and spatial evolution of the rupture process (e.g., Hartzell & Heaton 1983). They calculated the distribution of slip on two listric-thrust faults by combining geological information and focal mechanisms and using a combined inversion of the teleseismic waveforms and GPS coseismic displacements. The inversion shows that rupture started near the town of Yingxiu and propagated along the Yingxiu-Beichuan fault. The calculated slip distribution indicates large slip at depth on the Yingxiu-Beichuan fault, which coincides with field geological observations (X. Xu et al. 2009). Two significant slip patches are clearly shown in the slip distribution. The southern one, below Hongkou at depths between 10 and 15 km, shows a maximum slip between 10 and 12 m. The northern patch, which is between Beichuan and Pingtong, shows a slip of $\sim$12 m at shallow depth. The Tongji-Hanwang segment on the Guanxi-Jiangyou fault also ruptured for approximately 72 km with 5–6 m slip at depth. Along the Qingchuan segment of the Yingxiu-Beichuan fault, where the rupture does not reach the surface, 3–4 m slip is also inferred at depth.

To reveal details of the rupture processes associated with the Wenchuan earthquake, Y. Zhang et al. (2009) used a linear-inversion technique, assuming constant rupture velocity and fixed-source time functions of subevents, to image the spatial-temporal variation of the source mechanism based on 48 worldwide teleseismic waveforms. They show that the entire rupture process can be approximated as four successive subevents, with each breaking a different section of rupture zone (Y. Zhang et al. 2009). The first subevent characterizes the first 10 s of slip and ruptured $\sim$40 km of the fault with almost pure reverse faulting. It released approximately 7% of the total seismic moment, equivalent to a $M_w = 7.5$ event. The second subevent occurred between 10 s and 42 s with largely reverse slip plus a small right-slip component. It ruptured approximately 100 km and accounts for 61% of the total seismic moment. The third subevent ruptured a $\sim$60-km stretch of the fault with a large strike-slip component and released only 9% of the total seismic moment. The fourth subevent started 60 s after slip began and continued to the end of rupture (95 s from initiation), releasing 23% of the total seismic moment. Strike slip mostly occurred with a small reverse-faulting component along its length of approximately 110 km. The overall process includes a rupture that starts from the southwestern end as reverse faulting and propagates unilaterally northeastward for 300 to 340 km with an increasing strike-slip component (Y. Zhang et al. 2009).

SURFACE RUPTURES ASSOCIATED WITH THE WENCHUAN EARTHQUAKE

Postearthquake field investigations indicate that the 2008 Wenchuan earthquake occurred on multiple imbricate, high-angle (60° to 80°) reverse faults. The rupture zone consists of at least three strands (X. Xu et al. 2008, 2009): the NE-trending Yingxiu-Shuiguan rupture on the NE-trending Yingxiu-Beichuan fault, the Tongji-Hanwang rupture on the NE-trending Guanxian-Jiangyou fault, and the short, NW-trending, arcuate Xiaoyudong rupture that apparently intersects the Longmen Shan fault (**Figure 2**).

The Yingxiu-Shuiguan Rupture

For the Yingxiu-Beichuan fault, the primary structure responsible for the Wenchuan earthquake, the rupture started near the town of Yingxiu (30.986°N, 103.364°E); crossed towns and villages such as Hongkou, Gaochuan, Beichuan, Pingtong, and Nanba; and terminated east of Shuiguan (32.2862°N, 104.9515°E) with a length of 240 km (**Figure 2**). Discontinuous ruptures such as fissures and cracks could be found for an additional 20 km to the northeast, but no displacement could be measured along this northeastward continuation. For another ~60 km along the Yingxiu-Beichuan fault beyond the northeastern end of the surface rupture and fissuring zone, frequent aftershocks delineated an additional rupture segment that did not reach the surface (**Figure 2**). Also, southwest of the southwestern end of the mapped surface rupture, aftershocks extended for another ~20 km, which makes the total length of the aftershock zone—and presumably of the rupture itself—340 km (**Figure 2**).

Primarily reverse faulting characterizes the southern fault segment from Yingxiu to Xiaoyudong. At Yingxiu, the surface rupture cuts through the prosperous tourist town and caused significant damage and many casualties. A paved road on the terrace of the Minjiang river has been offset 2.2 ± 0.3 m vertically, but no horizontal offset has been observed (**Figure 3*a***). Northeastward approximately 10 km near Hongkou, the rupture displaced roads, farming fields, and farmers' houses to form prominent fault scarps. The vertical offsets increase to 4 to 5 m, and right-lateral displacements of 1 to 3 m were also measured. At one place (31.10472°N, 103.62225°E), the largest vertical offset of 6.2 ± 0.5 m of this segment was measured (X. Xu et al. 2009). A seismogenic scarp at Bajiao (31.14522°N, 103.69189°E) dips 76° northwestward, and slickenside striations on the fault surface indicate that the fault slipped at 75 to 82° subvertically (**Figure 3*b***). This testifies to a prominent component of reverse faulting.

North of the Xiaoyudong fault to Gaochuan, surface ruptures are present in the high mountains of Longmen Shan. Numerous landslides and earthquake lakes prohibited access to most of the places, so only four localities have been studied. The steep topography does not preserve surface ruptures, and only in flat valleys can ruptures be observed. The vertical offsets in this segment average 3 to 4 m with an average of ~2 m of right-lateral offset. For example, the surface rupture displaced a paved road 3.7 ± 0.3 m vertically and 0.55 ± 0.2 m right-laterally near the town of Qingping (31.34071°N, 104.06715°E) (**Figure 3*c***).

From north of Gaochuan to Shuiguan, the coseismic rupture occurred on a single fault, along which both maximum vertical and horizontal offsets occurred (**Figure 2**). At Beichuan and to its northeast, a subvertically dipping surface rupture offset ridges and gullies sharply in places to form scarps whose heights vary from 1–2 m up to ~9 m (**Figures 2*b*** and **3*d***). The maximum vertical offset is observed northeast of the town of Beichuan where the surface rupture cuts through a farmer's yard (**Figure 4*a,b***). Houses adjacent to the three-story building and to a flat, 8 m–wide yard were destroyed, as the rupture offset passed beneath both those houses and the yard

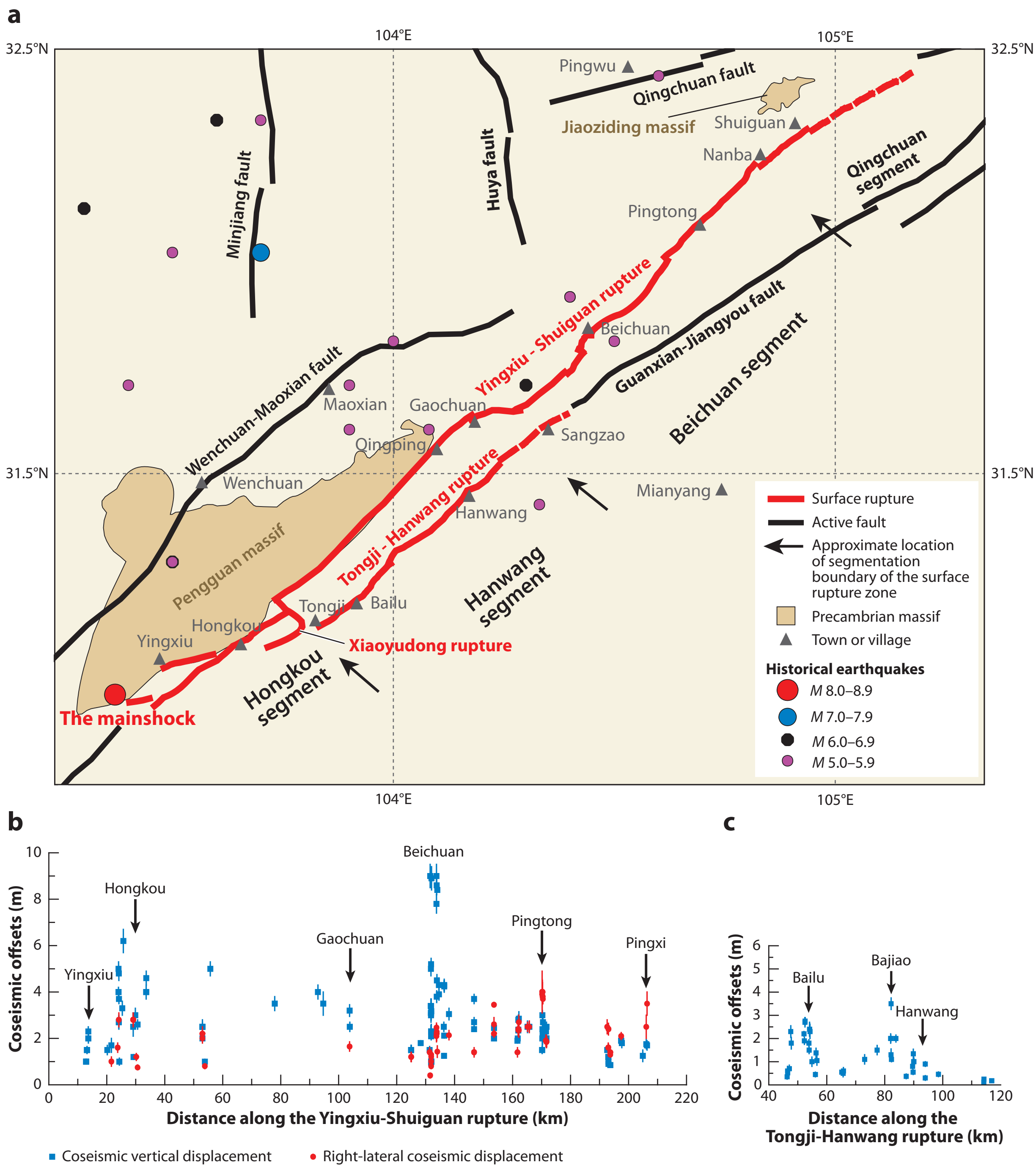

Figure 2

Surface ruptures and coseismic displacements associated with the 2008 Wenchuan earthquake. (*a*) Active faults and surface ruptures. (*b*), (*c*) Coseismic slip distributions along the Yingxiu-Beichuan fault and the Guanxian-Jiangyou fault, respectively.

Figure 3

Photos of surface ruptures associated with the Wenchuan earthquake. (*a*) Fault scarp formed during the earthquake at the town of Yingxiu near the southern end of the rupture zone. View is to the northwest. The road and the southern bank of the Minjiang river have been offset for 2.2 ± 0.2 m. A person standing at the foot of the scarp provides scale. (*b*) Subvertical fault scarp at Bajiao village near Hongkou town. Surface rupture shown in the photo dips 76° northwestward, and slickenside striations on the fault surface indicate that fault slipped at an angle of 75–82° subvertically. View is to the northeast. (*c*) Fault scarp near the town of Qingping, where a paved road has been offset 3.7 ± 0.3 m vertically with a minor right-lateral slip of 0.55 ± 0.2 m. View is to northwest. (*d*) Step-dipping fault scarp near the town of Beichuan. View is to the southwest. The scarp height is 1.8 ± 0.4 m. (*e*) Schoolyard at the town of Bailu, offset by the Tongji-Hanwang rupture. The yard was flat and the two buildings were the same height before the earthquake. The vertical displacement was measured to be 1.8 ± 0.3 m. View is to the northeast. (*f*) Vertical and left-lateral slips along the northwest-trending Xiaoyudong fault. A paved road is offset with left-lateral offset 2.3 ± 0.3 m and vertical offset of 1.5 ± 0.4 m.

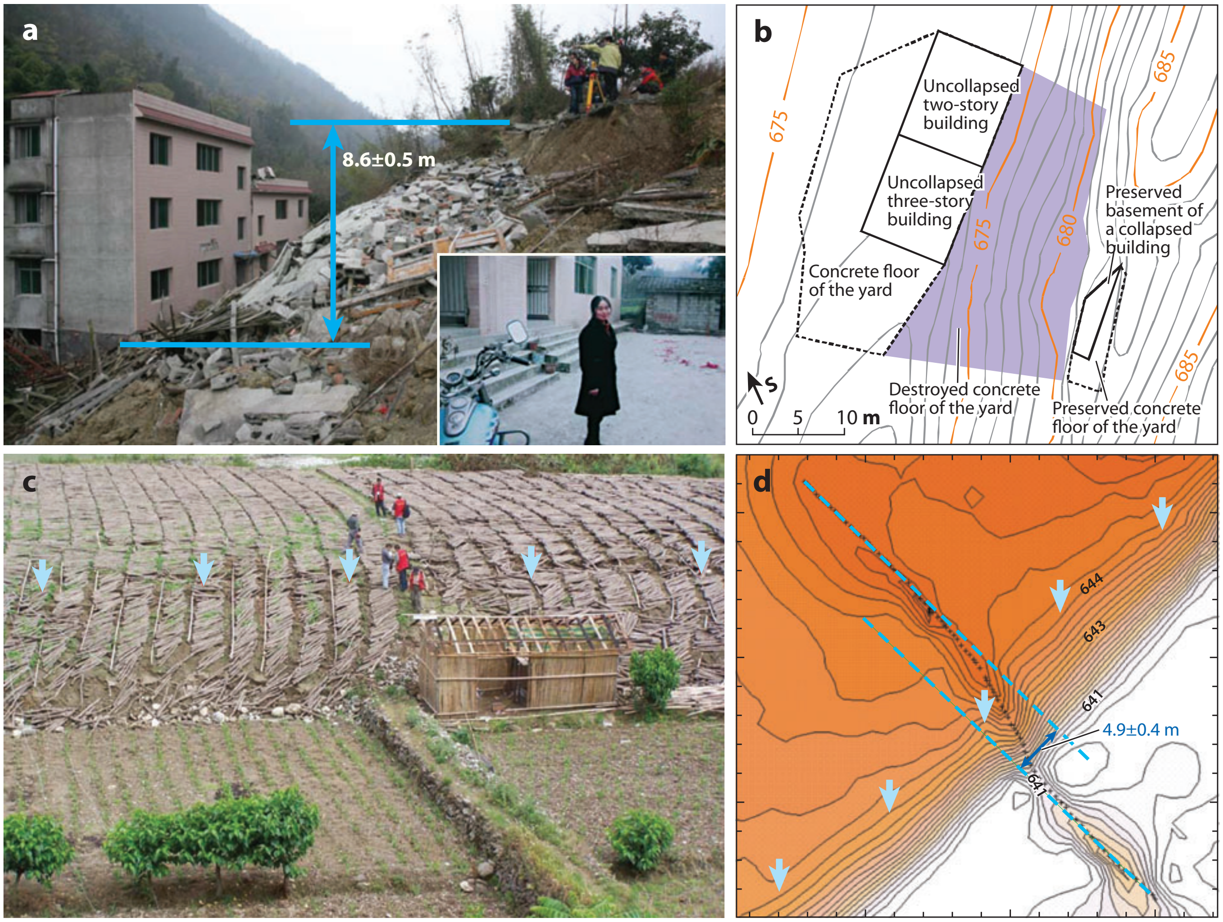

Figure 4

The maximum vertical and horizontal coseismic displacements. (*a*) A farmer's yard offset by the rupture. The inset photo shows the yard before the earthquake. The houses opposite the three-story building were destroyed as the rupture offset the flat and 8 m–wide yard. A portion of the yard has been preserved on the hanging wall (the concrete surface where survey equipment is located) after the earthquake. (*b*) Detailed total station map of the offset shown in (*a*). The separation of the preserved concrete yard from its counterpart in front of the building yields 8.6 ± 0.5 m of vertical offset. (*c*) The maximum right-lateral offset near the town of Pingtong. A small trail within a farming field has been offset for 4.0 ± 0.3 m right-laterally. (*d*) Total station map of the offset shown in (*c*).

(Ran et al. 2010). The inset photo shows the yard and three-story building before the earthquake (**Figure 4*a***). A portion of the yard has been preserved on the hanging wall (the concrete surface where survey equipment is shown in **Figure 4*a***). The separation of the preserved concrete yard from its counterpart in front of the building yields 8.6 ± 0.5 m of vertical offset (Ran et al. 2010). The maximum right-lateral offset is located near the town of Pingtong, where a small trail within a farming field has been offset 4.9 ± 0.3 m right-laterally (**Figure 4*c,d***).

Further northeastward, the right-lateral strike-slip component increases and becomes dominant at Pingtong and further northeast. For example, subvertically dipping surface ruptures are prominent at Pingxi ~4 km from the northern end of the surface rupture zone, where the vertical offset is 1.75 ± 0.25 m and the right-lateral slip reaches 3.0 ± 0.5 m.

The Tongji-Hanwang Rupture

Approximately 10 to 12 km southeast of and parallel to the Yingxiu-Shuiguan rupture, the Tongji-Hanwang rupture follows a section of the Guanxian-Jiangyou fault for 72 km (**Figure 2**). The rupture also dips northwestward with predominantly reverse motion (X. Xu et al. 2009). The rupture starts near the town of Tongji where scarp heights vary from 1 to 2 m without obvious horizontal offset. The vertical offset increases northeastward. At the town of Bailu, the rupture cuts through a schoolyard between two school buildings to form a prominent fault scarp (**Figure 3*e***). The measured scarp height is 1.8 $\pm$ 0.3 m with no horizontal offset. The nearest distance of the fault scarp to one of the school buildings is only 3 m. Fortunately, the buildings did not collapse and none of the more than 300 elementary-school students were even injured. Further northeast, X. Xu et al. (2009) reported a vertical offset of 3.5 m, which is the largest along this segment. The vertical offset remains approximately 1 m near the intensively damaged industrious town of Hanwang. The rupture terminates near the town of Sangzao with the scarp height decreasing to 0.2 to 0.3 m.

The Xiaoyudong Rupture

Northwest of the southwestern termination of the Tongji-Hanwang rupture is a 6 km–long, arcuate surface rupture named the Xiaoyudong rupture zone (**Figure 2**). This remarkable rupture is characterized by its change in strike from northeast in the southwestern part to north-northwest in the northeastern part. The north-northwest-trending section has a predominant left-slip component, whereas the north-northeast-striking section shows mostly reverse faulting. **Figure 3*f*** shows that the Xiaoyudong rupture offsets a paved road with a left-lateral offset of 2.3 $\pm$ 0.3 m and a vertical offset of 1.5 $\pm$ 0.4 m. The Xiaoyudong rupture apparently offsets the Yingxiu-Beichuan rupture zone left-laterally by approximately 4 km (**Figure 2**), and it aligns with the northwest-trending (and protruding) aftershock zone west of the town of Yingxiu (see below).

Geometric Segmentation and Slip Distribution

To summarize, the Wenchuan earthquake occurred by slip on multiple imbricate, high-angle (60–80°) reverse faults with right-lateral components of slip. The surface rupture is 240 km in length with a maximum vertical offset of ~9.0 m and a right-slip component of ~4.9 m. It is also evident that vertical components dominate the coseismic deformation except near the northeastern end where right-lateral strike slip becomes predominant (**Figure 2*b,c***). The entire rupture zone can be divided into four segments, each of which has a different geometric pattern and kinematic behavior (**Figure 2*a***). The geometric complexity as manifested by multisegmented and imbricate surface ruptures indicates structural discontinuities or barriers along the seismogenic fault that require complex rupture processes to overcome them (Sibson 1986, 1989; Zhang et al. 1991; Yeats et al. 1997). The four-segment nature coincides with teleseismic waveform-inversion results of temporal and spatial variations of the earthquake rupture (Ji 2008, Nishimura & Yagi 2008, Wang et al. 2008, Y. Zhang et al. 2008).

The envelopes of coseismic slip distribution along the ruptures corroborate the segmented geometric pattern of the zone (**Figure 2**). Each segment reveals a different pattern of slip distribution. The Hongkou segment has a single peak near its middle portion. The Hanwang segment involves slip partitioning between two parallel strands with a total average offset in the range of 6–8 m (**Figure 2**). The Beichuan segment has a peak vertical offset in its southern portion and a peak horizontal offset near its middle. The Qingchuan segment has no surface displacement.

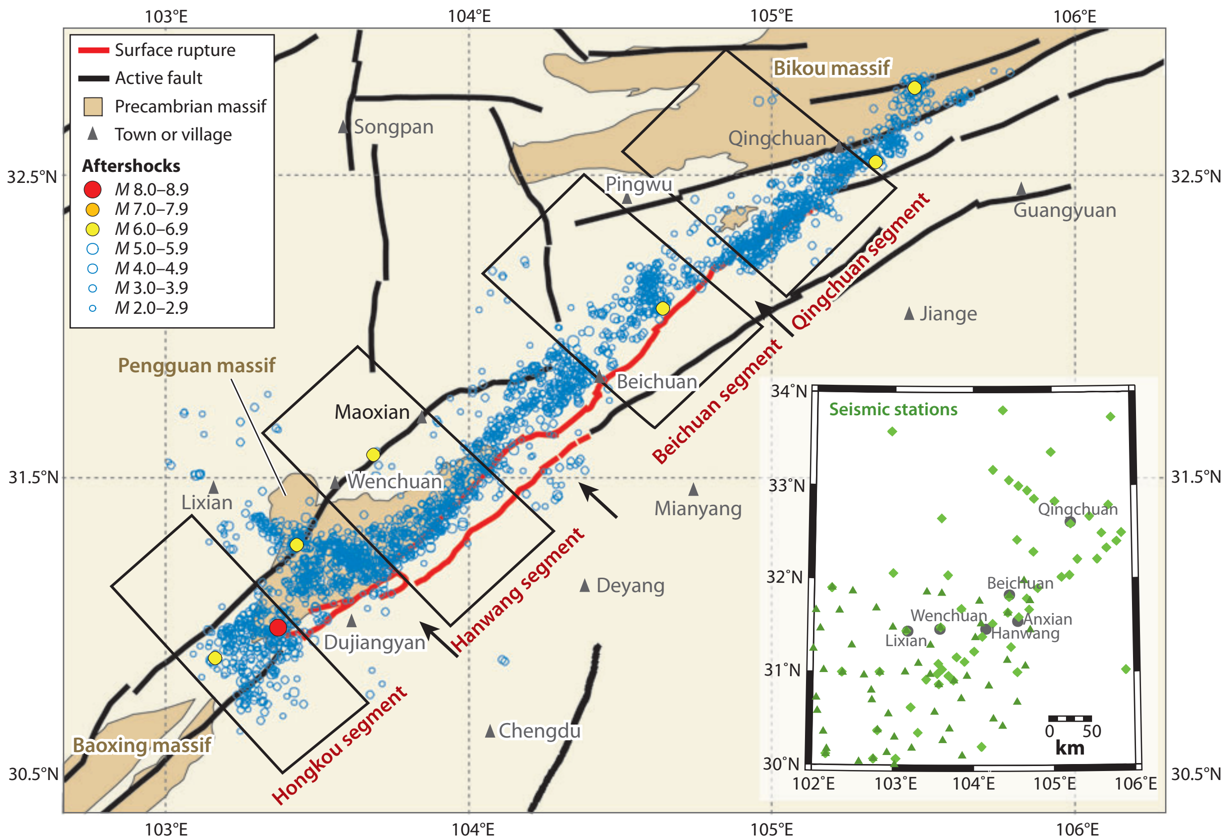

Figure 5

Relocated aftershock distribution of the Wenchuan earthquake. Boxes indicate aftershocks of each segment used to construct profiles in **Figure 6**. The lower-right inset shows distribution of seismic stations used for the aftershock relocations. Triangles are stations affiliated with the Western Sichuan Seismic Array (WSSA) deployed since 2007; diamonds are from the Sichuan Seismic Network and some temporary stations deployed after the mainshock.

AFTERSHOCK DISTRIBUTIONS AND THE STRUCTURAL PATTERN OF THE LONGMEN SHAN FAULT ZONE

Precise relocations of the aftershocks can illuminate subsurface structures of ruptures (e.g., Carena et al. 2002, Hauksson & Shearer 2005). As mentioned above, the mainshock occurred within the northeastern quadrant of the WSSA. The array also spans 2/3 of the aftershock zone. Together with the Sichuan Seismic Network and other seismic stations deployed immediately after the earthquake, the stations shown in **Figure 5** allow precise locations of the aftershocks. To avoid complications arising from other wave trains, Chen et al. (2009) used only stations within 100 km of the epicenter for relocations of each event and selected a total of 3920 events for relocation using the double-difference software hypoDD of Waldhauser & Ellsworth (2000). Each of these events was recorded by at least eight stations with a high signal-to-noise ratio. Finally, 3622 events were relocated with uncertainties estimated to be ± 0.85 km and ± 1.75 km for horizontal and vertical coordinates, respectively (Chen et al. 2009).

Unlike the 1999 Chi-chi earthquake in Taiwan, in which most of the aftershocks lie along a gently dipping zone for ~100 km in the hanging wall (Carena et al. 2002, Chang et al. 2007), most of the aftershocks are narrowly distributed within a zone 15–30 km wide in the hanging wall of the Yingxiu-Beichuan fault (**Figure 5**). The relatively narrow distribution offers no evidence of thin-skin thrust faulting. The overall pattern of the hypocenter distribution coincides with the segmented nature derived from surface ruptures (**Figure 5**), indicating how fault structure provides a geometric control on the aftershock distribution. Aftershocks in the Hongkou segment cluster within the main body of the Precambrian Pengguan massif and suggest the possibility of a high level of residual or redistributed stress after the mainshock. A northwest-trending aftershock zone cuts through the massif. In the Hanwang segment, most of the aftershocks occurred in the hanging wall of the Yingxiu-Beichuan rupture, and a minor portion occurred within the hanging wall of the Tongji-Hanwang rupture. The boundary between the Hanwang and Beichuan segments corresponds spatially to a broad region of aftershocks (**Figure 5**). Aftershocks along the Beichuan segment are mostly confined to the hanging wall of the earthquake rupture. The absence of aftershocks in the footwall along this segment implies that the rupture of the Guanxian-Jiangyou fault does not extend to this segment. In the Qingchuan segment, aftershocks occurred on both sides of—but close to—the northern extension of the Yingxiu-Beichuan fault (**Figure 5**). This pattern is similar to that along typical strike-slip earthquakes, such as the Loma Prieta (1989), Landers (1992), and Parkfield (2004) earthquakes in California (Sieh et al. 1993, Dietz & Ellsworth 1997, Thurber et al. 2006).

Most of the relocated aftershock hypocenters occurred between depths of 10 and 22 km (Chen et al. 2009). This pronounced depth distribution suggests that the elastically deformed brittle portion of the crust (schizosphere) may be as deep as 22 km, below which the brittle-ductile transition lies. It also suggests that significant coseismic slip takes place mainly at shallow depths above 10 km, so that previously accumulated stress was released during the mainshock. Studies of aftershock patterns and mainshock faulting indicate that the spatial distribution of aftershocks reflects either a continuation of slip in the regions with relatively small slip during the mainshock or the activation of subsidiary faults within the volume surrounding the boundaries of mainshock rupture (Ouyed et al. 1983, Mendoza & Hartzell 1988, Hatzfeld et al. 1997, Chang et al. 2007). In other words, aftershocks do not occur where the mainshock slip is large; instead, they occur in regions where the stress level is high following the mainshock. This relation may be used to delineate coseismic faults at depth. For strike-slip faults, the orientation of the aftershock clustering commonly delineates the seismogenic fault (Sieh et al. 1993, Dietz & Ellsworth 1997, Thurber et al. 2006). For reverse or thrust faults, the aftershocks mainly occur in the hanging walls with high residual stress, and the seismogenic fault is commonly devoid of aftershocks.

Figure 6 shows profiles of aftershock hypocenters across different segments of the Wenchuan earthquake rupture zone that illuminate subsurface seismogenic structures. Most of the aftershocks across the Hongkou segment lie in the depth range of 10 to 20 km within the imbricate structures, and only a few are sparsely located shallower than 10 km (**Figure 6*a***). The basal envelope of aftershocks may delineate the base of the schizosphere or brittle-ductile transition zone below which ductile shear accommodates strain. The mainshock took place initially on a ramp dipping northwestward at 30–40° in the depth range of 15 to 20 km, and at shallower depths the fault steepens to ~70° to form prominent surface ruptures with significant displacements along the Yingxiu-Shuiguan rupture. Eastward the earthquake broke another ramp splay to form the Tongji-Hanwang surface ruptures. Farther east, there may have been some minor slip on the range-front fault, but it did not reach the surface (**Figure 6*a***). Aftershocks on the Hanwang segment lie mainly in the depth range of 14 to 22 km between the Yingxiu-Shuiguan and Tongji-Hanwang rupture (**Figure 6*b***). Almost all the aftershocks along the Beichuan segment occurred in the depth range of 8 to 18 km, northwest of the Yingxiu-Shuiguan rupture and in the hanging wall (**Figure 6*c***). The

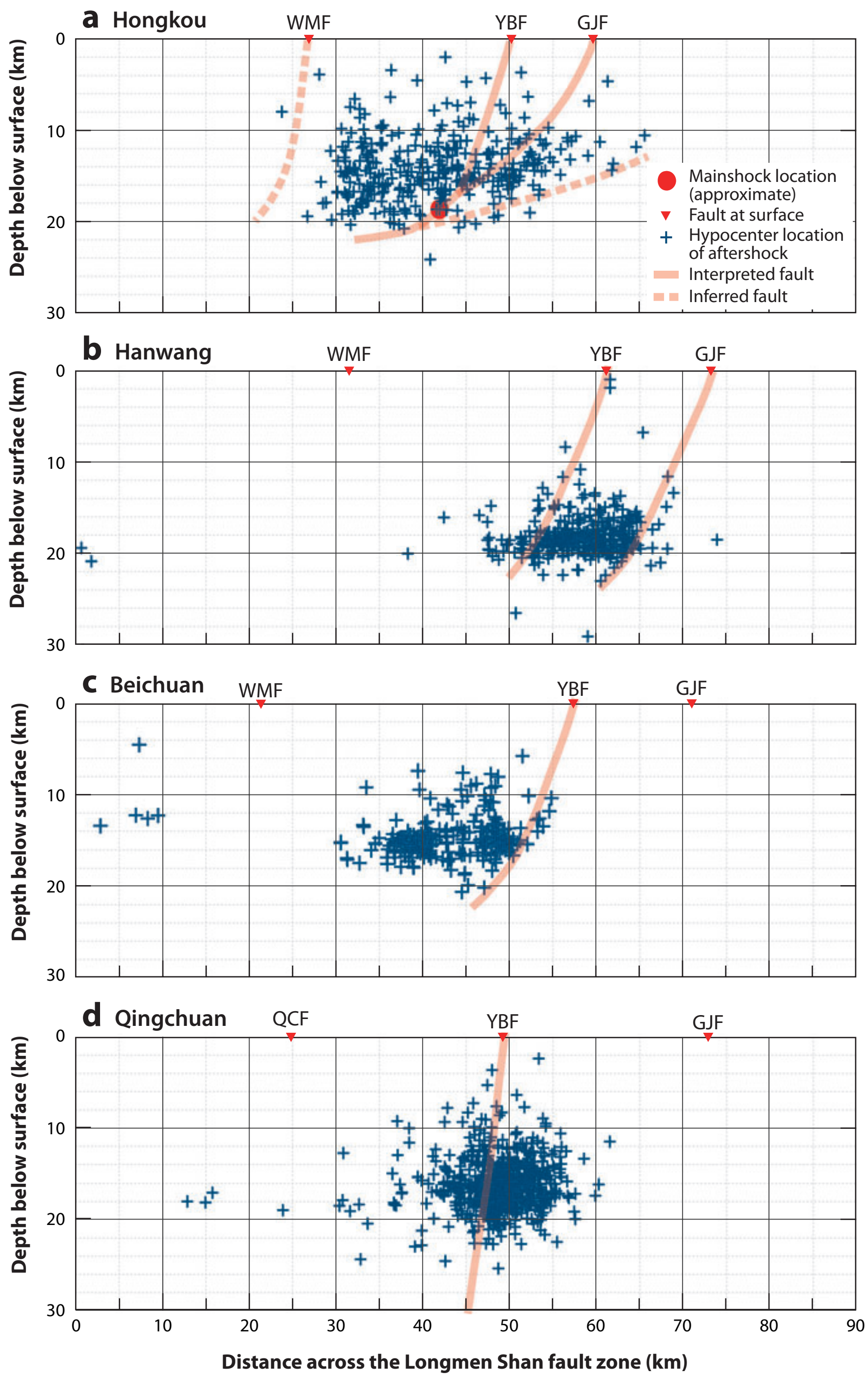

Figure 6

Distribution of relocated aftershocks across the Hongkou (*a*), Hanwang (*b*), Beichuan (*c*), and Qingchuan (*d*) segments. Locations of the profiles are shown in **Figure 5**. Solid lines are interpreted faults based on geological and seismological information. Dashed lines are inferred faults. Abbreviations: WMF, Wenchuan-Maoxian fault; YBF, Yingxiu-Beichuan fault; GJF, Guanxian-Jiangyou fault; QCF, Qingchuan fault.

inferred fault also shows a steep dip of ~70° above ~15-km depth and decreases to ~40° before merging to a subhorizontal brittle-ductile transition zone at ~20 km. In the Qingchuan segment, along which the rupture did not reach the surface, aftershocks cluster around the northeastern extension of the Yingxiu-Shuiguan rupture zone in the depth range of 8 to 22 km along the Yingxiu-Beichuan fault. Concurrent with the prominently strike-slip component inferred from seismological and geodetic observations (Wang et al. 2008, Y. Zhang et al. 2008, Shen et al. 2009), the cross section (**Figure 6*d***) shows the pattern associated with steeply dipping strike-slip faults (Sieh et al. 1993, Dietz & Ellsworth 1997, Hauksson et al. 2002, Hauksson & Shearer 2005, Thurber et al. 2006).

To summarize, the aftershock patterns reveal three important features. First, most aftershock hypocenters in the depth range of 10 to 22 km suggest that coseismic slip of the mainshock released most of the seismogenic stress buildup in the upper 10 km of depth. Second, both map and cross-section views of the aftershock distribution demonstrate a complex fault system that suggests an earthquake rupture cascading along multiple segments. Third, the geometric pattern of aftershock distribution appears to favor the high-angle, listric-reverse faults that root into a subhorizontal brittle-ductile transition below 20–22 km of depth.

Fault-plane solutions for 32 aftershocks of magnitude 5 and higher show a dominance of reverse faulting along the major part of the rupture zone, the Hanwang and Beichuan segments (Zheng et al. 2009). Fault planes of most of these events trend parallel to the surface rupture zone along the main strand, and dip 30–80° northwestward with focal depths ranging from 11 to 19 km. Horizontal projections of the P-axes of the fault-plane solutions show a consistent west-northwest trend, subperpendicular to the strike of the Yingxiu-Beichuan fault (Zheng et al. 2009).

Six of the seven fault-plane solutions of major aftershocks northeast of the surface rupture show strike-slip faulting; one of these nodal planes strikes parallel to the Yingxiu-Beichuan fault zone. This corroborates the increasing strike-slip displacement along the surface rupture toward the northeast, obtained through teleseismic waveform inversion of the mainshock (Ji 2008, Wang et al. 2008, Y. Zhang et al. 2009) and geodetic measurements of coseismic movement. The 15 fault-plane solutions near the southern end of the rupture also reveal reverse, strike-slip, and even normal faulting. We interpret the variety of styles and orientations of faulting to be the result of complexities in stress near the tip of a propagating rupture.

LARGE-SCALE COSEISMIC DISPLACEMENTS FROM GEODETIC OBSERVATIONS

The prominent feature of the displacement field measured with GPS (Working Group 2008) is horizontal shortening or convergence across the seismogenic Yingxiu-Beichuan fault (**Figure 7*a***). Northwest of the surface rupture, all stations moved eastward and southeastward in a frame of

Figure 7

Coseismic displacements measured by GPS and leveling. (*a*) Coseismic horizontal displacements measured by GPS in a frame of reference defined by their preearthquake locations (Working Group 2008). Arrows of different colors represent different magnitudes of GPS velocity. Thick black lines are surface ruptures associated with the 2008 Wenchuan earthquake. (*b*) Coseismic horizontal displacement profile across the surface rupture zone. Blue squares are components normal to fault, representing coseismic convergence. Green squares are components parallel to fault, representing coseismic right-lateral offsets. (*c*) Coseismic vertical displacements measured by leveling. The last preearthquake leveling was 1997. The uncertainty and the accumulating slip from 1997 to 2008 are insignificant compared with coseismic displacements of 4.7 to 0.5 m. The coseismic displacement scale is logarithmic.

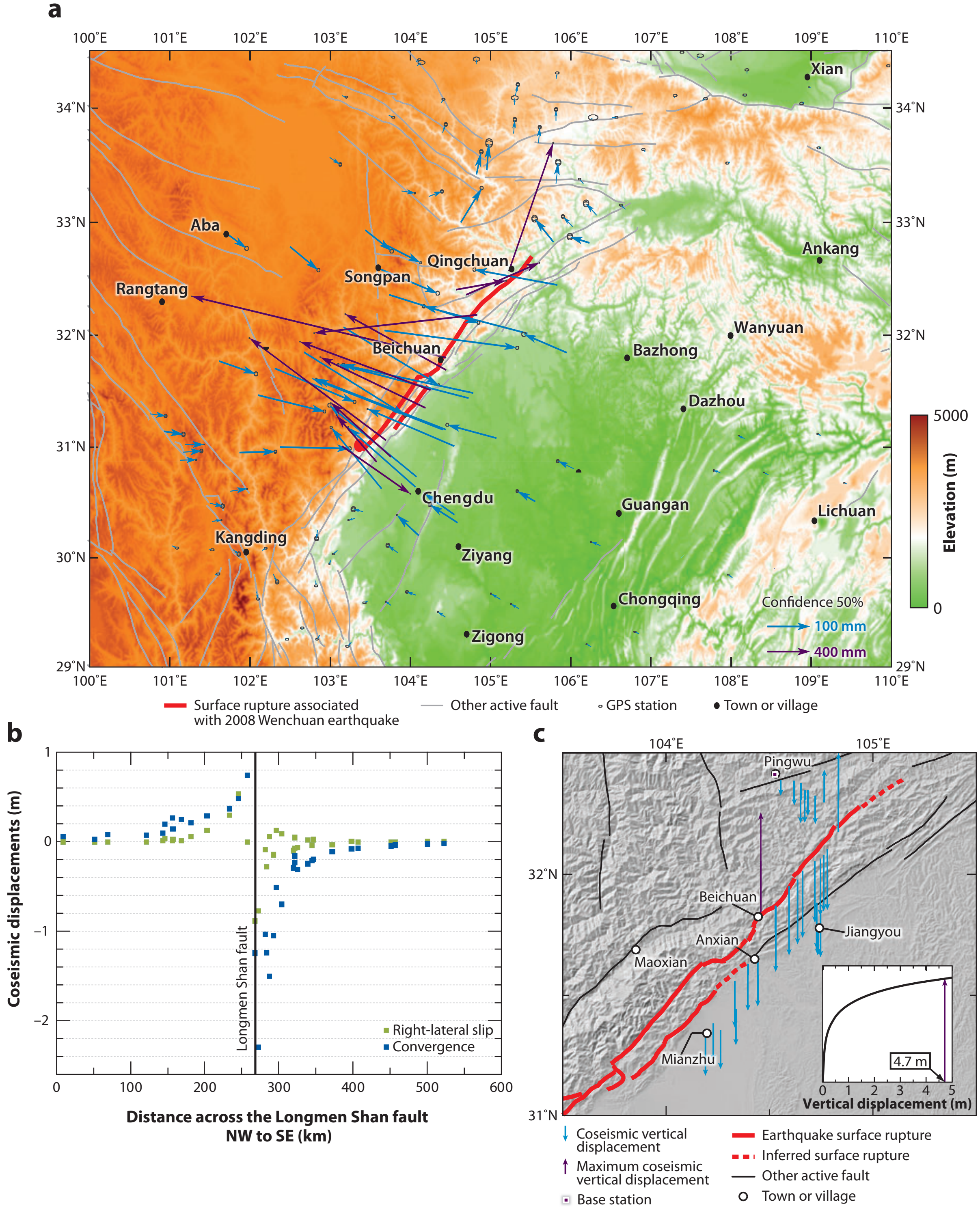
a
100°E 101°E 102°E 103°E 104°E 105°E 106°E 107°E 108°E 109°E 110°E
29°N 30°N 31°N 32°N 33°N 34°N
Xian
Aba
Ankang
Qingchuan
Songpan
Rangtang
Wanyuan
Beichuan
Bazhong
Dazhou
Chengdu
Guangan
Lichuan
Kangding
Ziyang
Chongqing
Zigong
Confidence 50%
100 mm
400 mm
5000
0
Elevation (m)
Surface rupture associated with 2008 Wenchuan earthquake
Other active fault
GPS station
Town or village
b
Coseismic displacements (m)
Longmen Shan fault
Right-lateral slip
Convergence
Distance across the Longmen Shan fault NW to SE (km)
c
104°E
105°E
32°N
31°N
Pingwu
Beichuan
Anxian
Jiangyou
Maoxian
Mianzhu
4.7 m
Vertical displacement (m)
Coseismic vertical displacement
Maximum coseismic vertical displacement
Base station
Earthquake surface rupture
Inferred surface rupture
Other active fault
Town or village

reference defined by their preearthquake locations, whereas stations located southeast of the rupture moved westward and northwestward. The observed maximum horizontal coseismic displacement is ~2.5 m west-northwestward at Station H035, which is only ~2 km from the fault on the footwall near the town of Beichuan (**Figure 7*a***). Unfortunately, there are no stations close to the fault on the hanging wall, which would have moved farther than that 2.5 m at the same distance from the fault trace but in the footwall. In the far field, the amount of displacement seems to decay at different rates on the two sides of the fault, with the hanging-wall displacement decaying more slowly. For example, Station H046, located ~120 km west of the fault on the hanging wall, moved 267 mm toward the fault, but the component perpendicular to the fault at Station JYAN, also located ~120 km east of the fault on the footwall, moved only 82 mm (**Figure 7*a***). This difference may reflect modest slip at depth within or below the brittle-ductile zone northwest of the rupture.

The right-lateral component of displacement associated with the Wenchuan earthquake is also apparent in the GPS displacement field (**Figure 7*b***). As is apparent from the displacements southeast of the fault, there is almost no strike-slip component along the southwestern segment of surface rupture; control points on opposite sides of the rupture moved toward one another. Like surface faulting measurements that indicate right-lateral slip of ~2–3 m along the central segment and 3–4 m along the northern segment (**Figure 2*b,c***), apparent components of right-lateral shear in the GPS field also increase to the northeast.

A leveling line across the northern part of the surface rupture zone was resurveyed after the earthquake (the last survey before the earthquake took place in 1997). The largest vertical displacement on the hanging wall is measured to be 4.7 m upward, at a site only 168 m from the fault in the town of Beichuan (**Figure 6*c***). The downward movement is 0.5 m at the maximum and decreases rapidly away from the fault on the footwall.

Although the coseismic displacement field can be roughly modeled by a simple elastic dislocation consisting of slip on a fault plane that dips at 70° in the upper 8 km, at 60° between 8 to 15 km, and at 40° between 15 to 20 km, the large misfit suggests that the deformation is too complex to be described by such a simple dislocation model. This problem partly arises from the sparse GPS control points, and especially from the lack of stations on the hanging wall near the fault. Employing a Newtonian nonlinear inversion method, Shen et al. (2009) used 362 GPS and 9110 InSAR control points to solve simultaneously for the fault geometry and slip distribution on segments of faults. The modeled rupture peaks at two places at shallow depth, one near Yingxiu and the other near Beichuan (**Figure 7**). Obviously, this spatial distribution of slip corroborates field observations in general (**Figure 2**).

The result of inverting the geodetic data again shows a complex fault geometry (**Figure 8**). To fit the GPS and InSAR data, the Yingxiu-Beichuan fault must dip to the northwest at a moderate average dip angle of ~43° near the southwest end, become steeper northeastward along the strike, reach a dip of ~50° at Nanba, and increase progressively until the fault plane becomes vertical

Figure 8

Geodetic inversion result: rupture geometry and coseismic slip distribution on fault (from Shen et al. 2009). The fault planes are viewed from southwest, at a 45° elevation angle in all diagrams. (*a*) Fault geometry. Fault-dip angle is assumed constant along dip and varies linearly along strike. (*b*) Coseismic slip distribution from inversion of GPS and InSAR data. The Guanxian-Jiangyou fault (GJF) is plotted away from its actual location. Black arrows show the slip vectors on the fault patches, whose amplitudes are denoted by the colors of the patches. Red lines are the mapped traces of surface breaks from X. Xu et al. (2009). The brown columns show the density of aftershocks along the fault, which occurred within 50 km of normal distance to the fault patches at the surface. B1–B11 and G1–G3 are fault segments on the Yingxiu-Beichuan fault and Guanxian-Jiangyou fault, respectively.

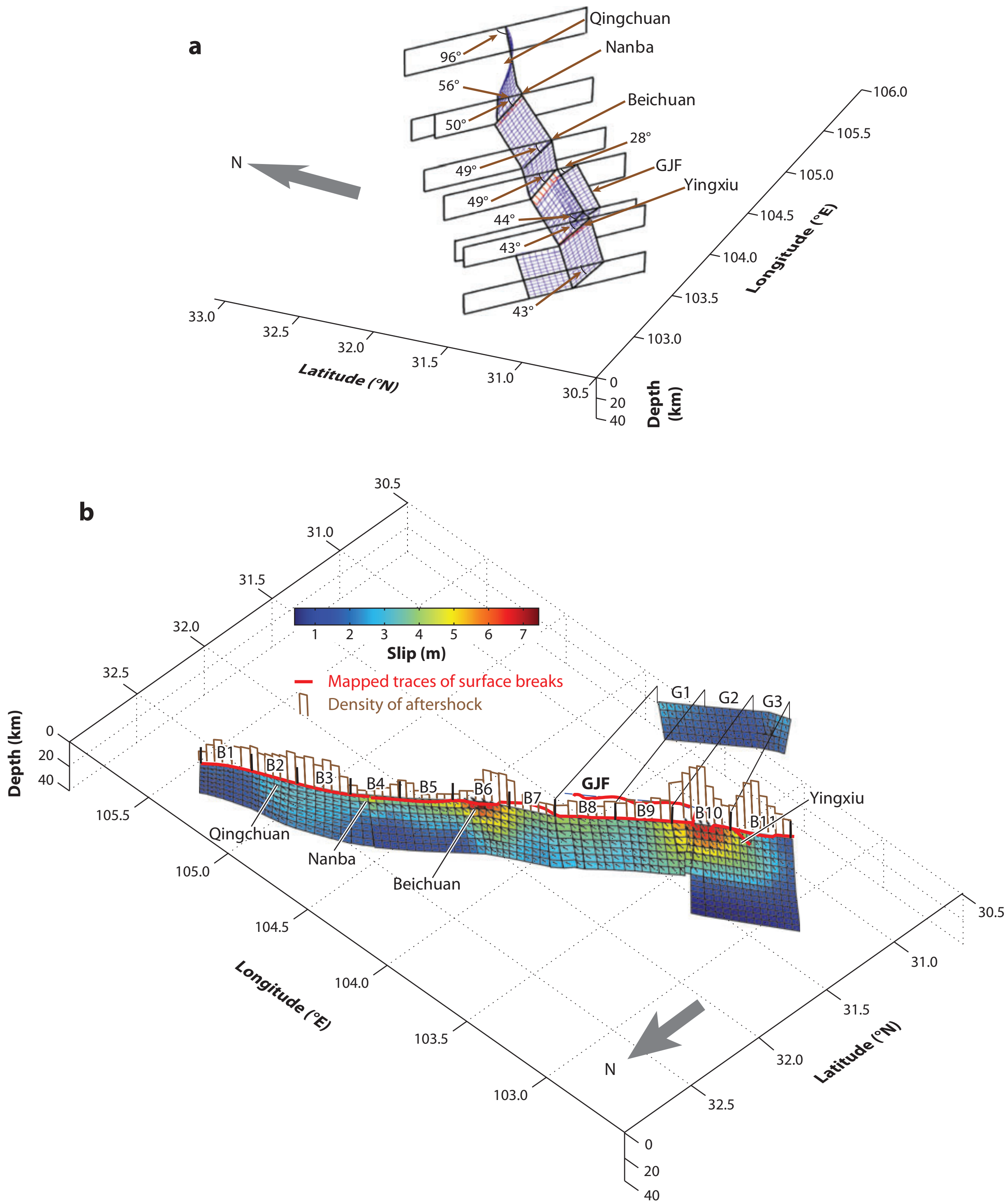

a
Qingchuan
Nanba
Beichuan
GJF
Yingxiu
N
96°
56°
50°
49°
49°
44°
43°
43°
28°
Latitude (°N)
33.0
32.5
32.0
31.5
31.0
30.5
Longitude (°E)
106.0
105.5
105.0
104.5
104.0
103.5
103.0
Depth (km)
0
20
40
b
Slip (m)
1 2 3 4 5 6 7
Mapped traces of surface breaks
Density of aftershock
G1
G2
G3
GJF
B1
B2
B3
B4
B5
B6
B7
B8
B9
B10
B11
Yingxiu
Qingchuan
Nanba
Beichuan
Depth (km)
0
20
40
Longitude (°E)
105.5
105.0
104.5
104.0
103.5
103.0
Latitude (°N)
30.5
31.0
31.5
32.0
32.5
N

at the northeast end of the rupture (Shen et al. 2009). Thus, in accordance with the geological observations and seismological inferences, high-angle, oblique reverse faulting is required to produce the geodetically observed coseismic displacement field. The segmented nature of geodetically modeled ruptures also coincides with geological segmentation along the fault zone (**Figures 2** and **5**) and attests to the fact that the Wenchuan earthquake broke through several high-slip junctions that connect major fault segments in a cascading rupture (**Figure 8**). These connecting structures may represent barriers that rarely fail, and do so only after high stress has accumulated after multiple rounds of smaller events have broken the adjoining individual segments (Shen et al. 2009). Such a cascading rupture scenario helps explain why Yingxiu, Beichuan, and Nanba experienced the highest shaking intensity of XI on the China Seismic Intensity Scale and suffered the greatest damage among the towns located along the fault zone.

IMBRICATE, LISTRIC, HIGH-ANGLE, OBLIQUE-SLIP FAULTING AND SEISMOGENIC STRUCTURES

Despite abundant seismic reflection data available in the Sichuan basin from the petroleum exploration, the deep structure of the Longmen Shan fault zone responsible for the Wenchuan earthquake generation is still not well known. The steep topography across the Longmen Shan prevents acquisition of high-resolution seismic data. The upper crustal structure of the Longmen Shan fault zone thus has been inferred from surface geology, a few shallow-level (less than 10 km–deep) seismic reflection profiles, and other geophysical data (Burchfiel et al. 2008, Zhu 2008, Hubbard & Shaw 2009). In the following we provide further evidence showing high-angle, listric-reverse faulting during the Wenchuan earthquake to shed some light on deep structure and processes that produced and supported the Longmen Shan Mountains.

Surface exposures of the earthquake rupture along the Yingxiu-Beichuan fault show dip angles of 70–80° to the northwest (**Figure 3*b*,*d***, for example) and 40–60° to the northwest along the Guanxian-Jiangyou fault (H. Li et al. 2008; Liu et al. 2008; X. Xu et al. 2008, 2009; Z. Xu et al. 2008). Trench excavations across the ruptures also reveal high-angle reverse faulting near the surface (Ran et al. 2008). For example, a 4 m–deep trench at Bajiao (31.14522°N, 103.69189°E) confirms a 76° dipping fault plane shown by **Figure 3*b*** along the Yingxiu-Beichuan fault; a 10 m–deep trench at Bailu across the Guanxian-Jiangyou fault shows a 47° dipping fault plane. Although the general consensus is that surface fault scarps are notoriously poor indicators of subsurface fault dip, they nevertheless serve as counterexamples to support high-angle rupture at least at the surface.

Z. Xu (2009) has led a project involving deep drilling of the Wenchuan earthquake rupture. Test drilling was conducted at Bajiao near the outcrop of the surface rupture with clear slickenside striations (**Figure 3*b***). The drill hole reaches the earthquake fault at a depth of 650 m as predicted by assuming a 70° dip of the fault plane (Z. Xu 2009) and therefore testifies to high-angle faulting extending to a depth of at least 650 m.

Fault-zone trapped waves are the wave trains that propagate within the fault zone and that follow the S waves on seismograms, usually with large amplitudes and low frequency (2–5 Hz) (Li & Leary 1990, Li et al. 1994). Fault-zone trapped waves have provided a powerful tool for revealing the subsurface geometry and physical properties of seismogenic fault zones and have been successfully exploited in studies of seismogenic faults of the Landers (1992), Hector Mine (1999), and Parkfield (2004) earthquakes (Li et al. 1994, 2002, 2006) as well as the Kunlun (2001) earthquake in the northern Tibetan Plateau (S.L. Li et al. 2005, Wang et al. 2009). Shortly after the Wenchuan earthquake, four densely instrumented, temporary seismic arrays were deployed

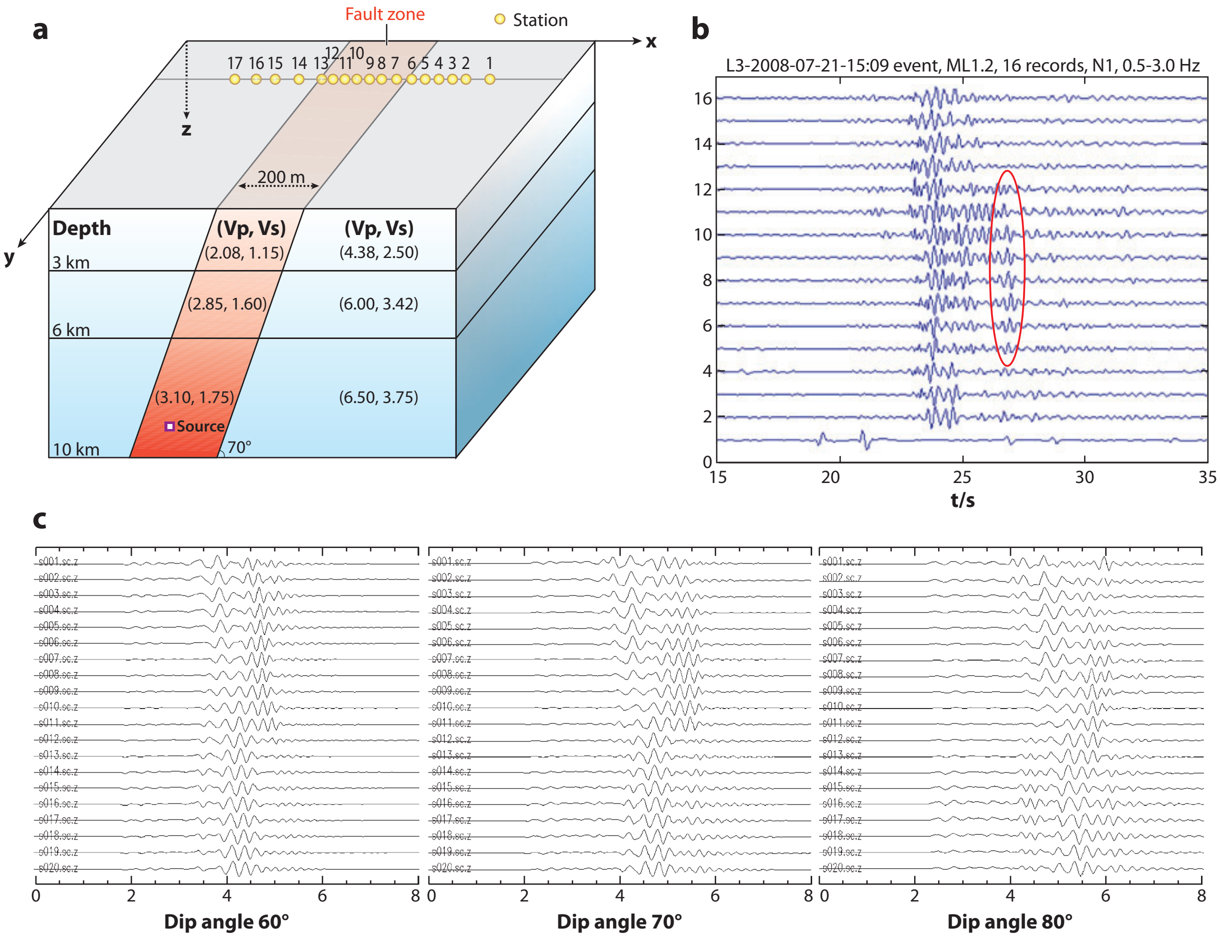

Figure 9

Fault-zone trapped waves across the Yingxiu-Beichuan fault zone (from S.L. Li et al. 2009). (*a*) Diagram summarizing parameters and properties of the fault zone. (*b*) Filtered seismic waveforms. The wave trains circled by a red ellipsoid are the observed fault-zone trapped waves. (*c*) Synthetic seismograms of the fault-zone trapped waves for dip angles of 60, 70, and 80°.

across the Yingxiu-Beichuan and the Guanxian-Jiangyou faults to record fault-zone guided waves (S.L. Li et al. 2009). Through waveform analysis and synthetic seismogram calculation, S.L. Li et al. (2009) found that the seismic velocity inside the fault zone is approximately one half of that of the host rocks. The widths of the rupture zone are approximately 200–230 m and 170–200 m across the southern and northern portions, respectively. To produce the recorded fault-zone trapped waves along each array, the southern portion (near Hongkou) of the fault zone must dip ~70° northwestward and the northern portion (near Pingtong) should dip even more steeply at ~80° northwestward (**Figure 9**). Fault-zone trapped waves can detect structures only above the aftershock depth, which is approximately 10 km. Thus, the Yingxiu-Beichuan fault apparently dips at 70 to 80° northwestward to a depth of 10 km.

Geological studies (Burchfiel et al. 1995, 2008; Chen & Wilson 1996; Wang & Meng 2008) and limited seismic reflection profiles from petroleum exploration (Chen et al. 2005, Jia et al.

2006, Hubbard & Shaw 2009) show that the Mesozoic to early Cenozoic structures of the Longmen Shan are characterized by a low-angle, imbricate thrust sequence of the Longmen Shan fault zone, where older faults have been rotated in the hanging walls of younger, listric faults that rise from a gently dipping brittle-ductile transition zone. Eastward, the base of the schizosphere, or brittle-ductile transition zone, merges upward with subhorizontal décollement beneath the Sichuan basin and finally ramps up in the Longquan Shan east of Chengdu (Chen et al. 2005, Jia et al. 2006, Burchfiel et al. 2008, Hubbard & Shaw 2009). As mentioned above, deformation within the Longmen Shan began during Late Triassic and Jurassic time and continued to early Cenozoic time (Burchfiel et al. 1995, 2008; Wang & Meng 2008). Late Cenozoic deformation as manifested by the Wenchuan earthquake has been proposed to result from eastward growth of the Tibetan Plateau as a consequence of lower crustal flow (Royden et al. 1997, 2008; Clark & Royden 2000; Kirby et al. 2002; Clark et al. 2005). Thus, geodynamic processes of late Cenozoic and present-day deformation appear to differ from those of Mesozoic and early Cenozoic deformation. It is possible that the style of late Cenozoic deformation has changed to high-angle, listric-reverse faulting with variable components of right-lateral strike slip and crustal shortening. In any case, low-angle thrust faulting is not the style of deformation seen from the late Cenozoic to the present. The 2008 Wenchuan earthquake and perhaps the abrupt topographic front of the Longmen Shan are manifestations of this new style of deformation.

The low-angle nature of the Longmen Shan faults revealed in seismic reflection profiling does not match the various observations associated with the Wenchuan earthquake mentioned above, all of which suggest a 70 to 80° dip angle above a depth of at least 10 km. As we mention above, aftershock hypocenter distributions appear to require that seismogenic faults dip steeply (more than 70° to the northwest) above ~15 km, become gently dipping (30 to 40°) only below ~15 km, and finally root into subhorizontal basal schizosphere (brittle-ductile transition zone) below 20 to 22 km (**Figure 6**). Regional seismicity from 1970 to 2008 in the western Sichuan and aftershocks of the Wenchuan earthquake (**Figure 10**) do not delineate an active low-angle thrust system as the 1999 Chi-chi earthquake aftershocks did in central Taiwan (Carena et al. 2002, Chang et al. 2007). Rather, microearthquakes seem to occur within the entire upper and middle crust (schizosphere) between depths of 10 and 25 km (**Figure 10**).

Fault-plane solutions of mainshock indicate slip on a fault dipping 30° to 40° (CENC 2008; Ji 2008, Nishimura & Yagi 2008, Y. Zhang et al. 2008, Global CMT Project). The precisely relocated epicenter of mainshock is only 8 km southwest of the primary surface rupture, the Yingxiu-Shuiguan rupture on the Yingxiu-Beichuan fault. If the earthquake rupture took place on a planar fault dipping 30 or 40°, for the given mainshock hypocenter location the surface rupture should appear 22–32 km east of the Yingxiu-Shuiguan rupture and within the Sichuan basin. Together, the relocated hypocenter and the fault-plane solution of mainshock require slip on a high-angle, listric-reverse fault to produce the mapped surface ruptures along the Yingxiu-Beichuan and Guanxian-Jiangyou faults.

We propose that the structure responsible for the Wenchuan earthquake consists of imbricate, oblique, high-angle, listric-reverse faults. The faults dip ~70° above 15-km depth, then dip 30 to

Figure 10

Comparison of seismic pattern of the western Sichuan with middle Taiwan and Southern California. (*a*) Background seismicity (*blue dots*) of the western Sichuan region from 1970 to 2008; aftershocks associated with the 2008 Wenchuan earthquake (*red crosses*). (*b*) Cross section of earthquake distribution for the area indicated in (*a*).

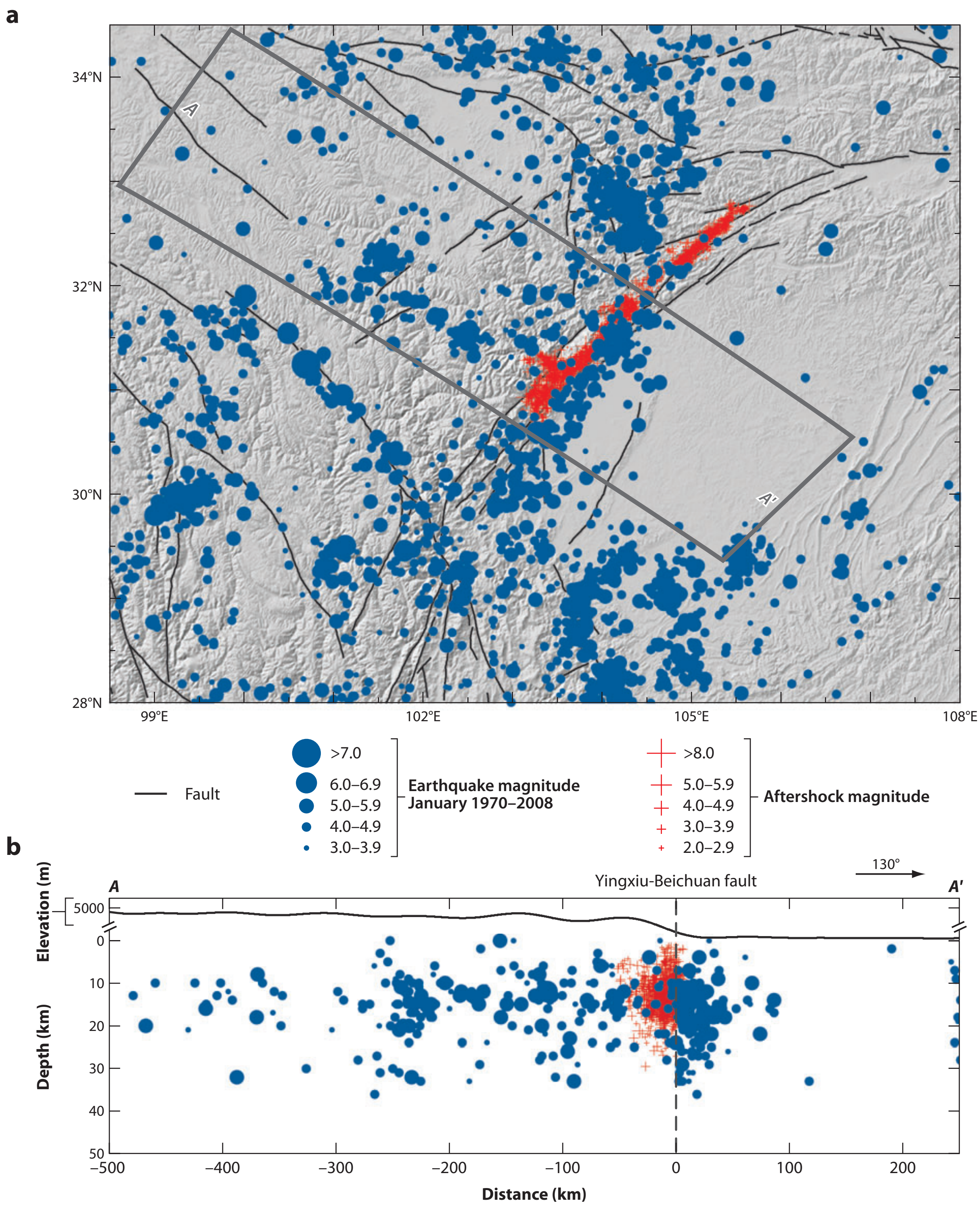
a
34°N
32°N
30°N
28°N
99°E
102°E
105°E
108°E
A
A'
Fault
>7.0
6.0–6.9
5.0–5.9
4.0–4.9
3.0–3.9
Earthquake magnitude
January 1970–2008
>8.0
5.0–5.9
4.0–4.9
3.0–3.9
2.0–2.9
Aftershock magnitude
b
Elevation (m)
5000
Depth (km)
0
10
20
30
40
50
A
A'
Yingxiu-Beichuan fault
130°
–500
–400
–300
–200
–100
0
100
200
Distance (km)

40° below ~15-km depth, and presumably root into the subhorizontal brittle-ductile transition zone below a depth of 20 to 22 km. Under the stress regime of pure shear, slip on a fault dipping 30–40° is easy, according to various fracture criteria. The initial slip on the gentle dipping fault probably caused the Coulomb stress changes that may in turn have triggered significant slip on the high-angle dipping fault above it to form the Wenchuan earthquake. The earthquake occurred on multisegmented ruptures, each of which is characterized by a different, complex geometry. The distribution of slip during the Wenchuan earthquake rupture presumably characterizes the style of late Cenozoic tectonic deformation of the Longmen Shan and eastern Tibet. It also helps explain the presence of a steep mountain relief (>4 km) with negligible coeval foreland subsidence.

THE WENCHUAN EARTHQUAKE RUPTURE AND PRESEISMIC ACCUMULATION OF STRAIN

The 2008 Wenchuan earthquake is a consequence of interactions among multiple geological units under a tectonic background in which the eastward growth of the Tibetan Plateau has been impeded by the tectonically stable Sichuan basin (Burchfiel et al. 1995, 2008; Royden et al. 1997; Clark & Royden 2000; Clark et al. 2005). The rheologically "soft" material in the middle and lower crust of eastern Tibet (Royden et al. 1997, 2008; Clark & Royden 2000; Clark et al. 2005; Liu et al. 2009) has been thickened, while the brittle upper crust has been obliquely pushed against the effectively rigid Sichuan basin on a high-angle reverse contact, the Longmen Shan fault zone.

Unlike an earthquake resulting from strain accumulation along a single fault, the Wenchuan earthquake involved three geological units: eastern Tibet, the Longmen Shan, and the Sichuan basin (P.Z. Zhang et al. 2009) (**Figure 11**). Interactions among them caused strain accumulation in the Longmen Shan, and the strain was eventually released to form during the devastating Wenchuan earthquake. The three units behave differently during both interseismic and coseismic periods.

The entire crust of eastern Tibet appears to be relatively weak (Wang et al. 2007; Yao et al. 2008; L. Xu et al. 2007; Liu et al. 2009) and thus serves as a deforming unit. During interseismic periods, significant deformation occurs mainly in eastern Tibet by convergence perpendicular to the Longmen Shan, right-lateral shear, and vertical movement (**Figure 11*a***). Thus eastern Tibet functions as a strain-energy conveyor belt that continuously transfers its deformation into accumulating stress on the Longmen Shan fault zone.

The Longmen Shan thrust sheet consists of Precambrian metamorphosed crystalline basement with relatively high strength such as the Baoxing, Pengguan, and Jiaoziding massifs (Burchfiel et al. 2008, Wang & Meng 2008, Z. Xu et al. 2008). These massifs are oriented in a direction unfavorable for slip; shortening normal to the strike of a high-angle reverse fault should increase its frictional resistance to prohibit slip. The region around the fault thus serves as a stress-accumulation unit (**Figure 11*a***) (P.Z. Zhang et al. 2009). The imbricate, listric, high-angle Longmen Shan fault zone remains locked during interseismic periods and accumulates stress at a low rate before an earthquake, so that preearthquake slip also accumulates slowly. During coseismic time, when the accumulated stress exceeds the critical strength of the Longmen Shan fault zone, an earthquake occurs to release huge amounts of strain energy that have been slowly stored during the several thousand–year interseismic period. The coseismic deformation occurs mostly in the interseismically locked Longmen Shan (**Figure 11*b***).

The Sichuan basin has behaved as a stable geological block since the late Mesozoic. It has a mechanically strong lower crust and upper-mantle structure (Wang et al. 2007, Liu et al. 2009) and

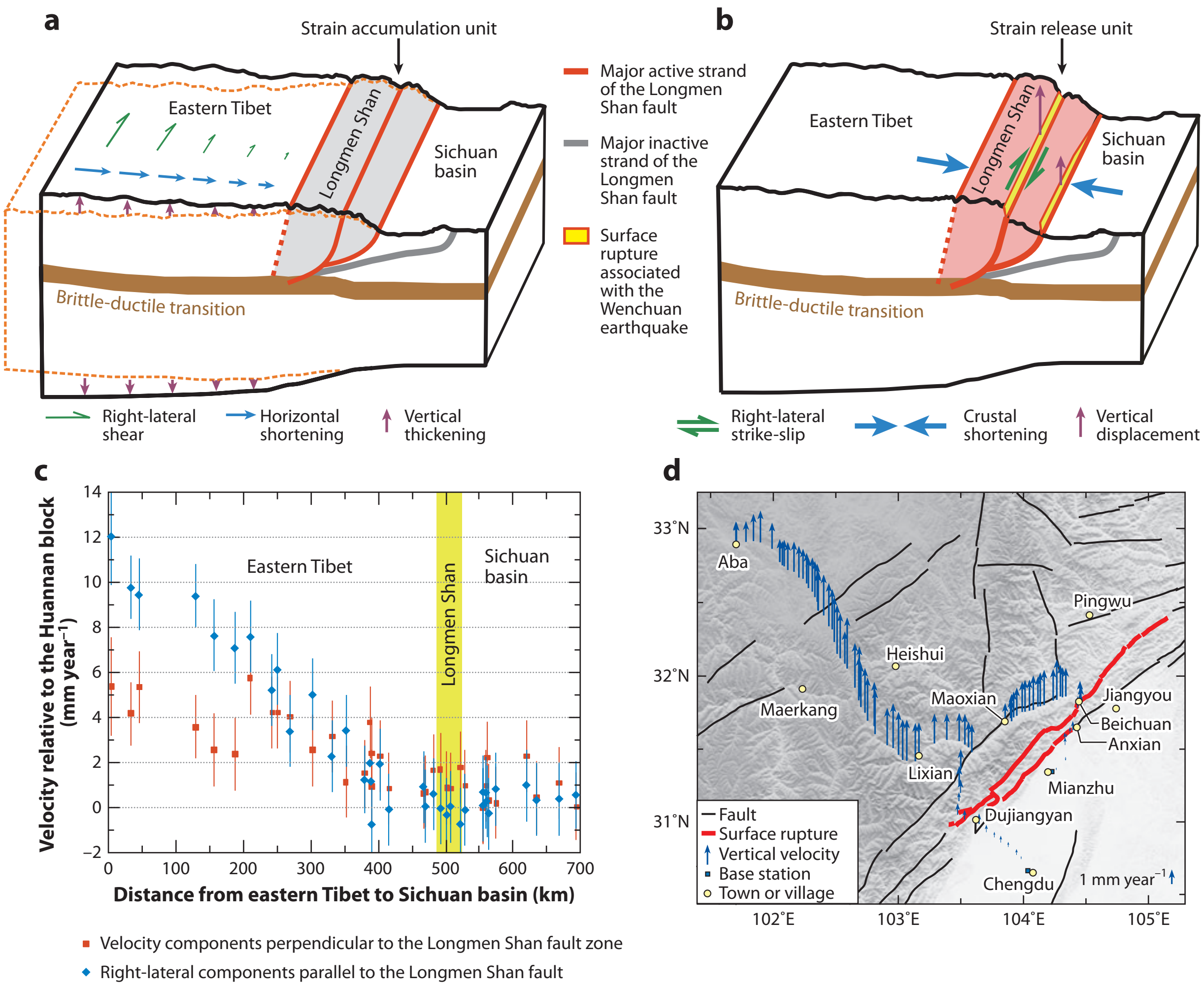

Figure 11

Preearthquake geodetic deformation and postulated cartoon model of the Wenchuan earthquake occurrence. (*a*) Diagram illustrating configuration of preearthquake deformation. Eastern Tibet has been shortened, wrenched, and uplifted to accumulate strain, while the Longmen Shan has been locked to accumulate stress. (*b*) Diagram showing coseismic configuration. The stress accumulated during the interseismic interval in the Longmen Shan is released through the Wenchuan earthquake rupture. (*c*) Preearthquake GPS velocity profile from eastern Tibet to the Sichuan basin across the Longmen Shan fault zone. (*d*) Vertical movement observed by leveling surveys along lines from Aba to Chengdu and from Maoxian to Mianzhu. The first survey was taken in 1976, and the last was in 1997. The uncertainty associated with the rates should be regarded to larger than ± 1 mm year^{-1}.

thus acts as a supporting unit to resist eastward movement of both eastern Tibet and the Longmen Shan (**Figure 11*a***). The supporting unit is a necessary condition for stress accumulation in the Longmen Shan fault zone, although minor deformation locally occurs along the western edge of the Sichuan basin.

Given the unique aspects of the Wenchuan earthquake—namely its size and occurrence in a region of modest displacement rates—it is important to understand how the preseismic accumulation of strain occurred in the locking unit (the Longmen Shan). **Figure 11*c*** shows preearthquake

GPS velocity profiles with respect to the Sichuan basin. It is evident that no more than 2–3 mm year^{-1} of relative motion occurs between the Longmen Shan and the Sichuan basin across the Longmen Shan fault (King et al. 1997, Shen et al. 2005, Gan et al. 2007, P.Z. Zhang 2008), which is consistent with geological slip rates of less than 2 mm year^{-1} (Densmore et al. 2007, Zhou et al. 2007). Instead, linear gradients of both components of velocity across eastern Tibet manifested themselves as continuous compressive strain and right-lateral shearing before the earthquake with rates of 4–5 and 7–9 mm year^{-1}, respectively, but distributed across a zone at least 500 km wide (**Figure 11*c,d***). An important question is what fraction of this geodetically measured accumulating strain in eastern Tibet is converted to seismogenic loading on the locking unit (the Longmen Shan). In other words, is the strain in eastern Tibet permanent, or could it be elastic?

Suppose that deformation rates (8.1–10.3 mm year^{-1}) in eastern Tibet were elastic and loaded the Longmen Shan. In that case, the slip rate of the Longmen Shan fault zone would be significantly larger than the rate of ~2 mm year^{-1} obtained by studies of active faulting. The average coseismic displacement of ~5 m (X. Xu et al. 2009) and a slip rate of ~2 mm year^{-1} suggest a recurrence interval of ~2500 years, which agrees with preliminary paleoseismic studies (P.Z. Zhang et al. 2008, Ran et al. 2008). Thus, the observations of fault slip rate and paleoseismology of the Longmen Shan fault zone imply that a large portion of strain in eastern Tibet must be permanent. On the other hand, background seismicity before the Wenchuan earthquake (**Figure 10**) showing a relatively dense distribution in eastern Tibet and almost a vacancy in the Longmen Shan further suggests that a large portion of preseismic strain is accommodated by permanent deformation or by energy released seismically on faults in eastern Tibet.

Coseismic deformation also provides a test of whether the strain in eastern Tibet is permanent or elastic because elastic strain would imply significant coseismic deformation and strain release. Coseismic deformation associated with the Wenchuan earthquake, in fact, takes place mostly within the interseismically locked Longmen Shan fault zone. As shown in **Figure 7**, geodetically measured regional coseismic deformation occurs mainly in the Longmen Shan and attenuates rapidly toward both eastern Tibet and the Sichuan basin. This is also the case for the deformation field obtained by InSAR (Sun et al. 2008, Shan et al. 2009). Aftershocks are confined within the Longmen Shan fault zone, along which the high intensities of X and XI on the China Seismic Intensity Scale are narrowly distributed, and decay rapidly away from it (**Figure 12*a***). Strong ground-motion data (X. Li et al. 2008) show that most of the stations that recorded peak ground acceleration in excess of 400 gal are located within the Longmen Shan region (**Figure 12*b***). Therefore, the eastward growth of the Tibetan Plateau probably causes significant permanent deformation in eastern Tibet, and only a small fraction of strain is loaded slowly onto the Longmen Shan fault zone. The combination of interseismic locking, relatively high strength, and slow loading in the Longmen Shan fault produces a great earthquake with a long recurrent interval occurring in a region of slow strain accumulation. The 2008 Wenchuan earthquake is an example of such an event and is likely to characterize the behavior of earthquakes that rupture the Longmen Shan fault zone.

Figure 12

Seismic intensity and strong ground motion of the 2008 Wenchuan earthquake. (*a*) Map showing that high seismic intensity and aftershocks are confined with the Longmen Shan fault zone. (*b*) Distribution of components of Peak Ground Acceleration (PGA) across the Longmen Shan fault zone.

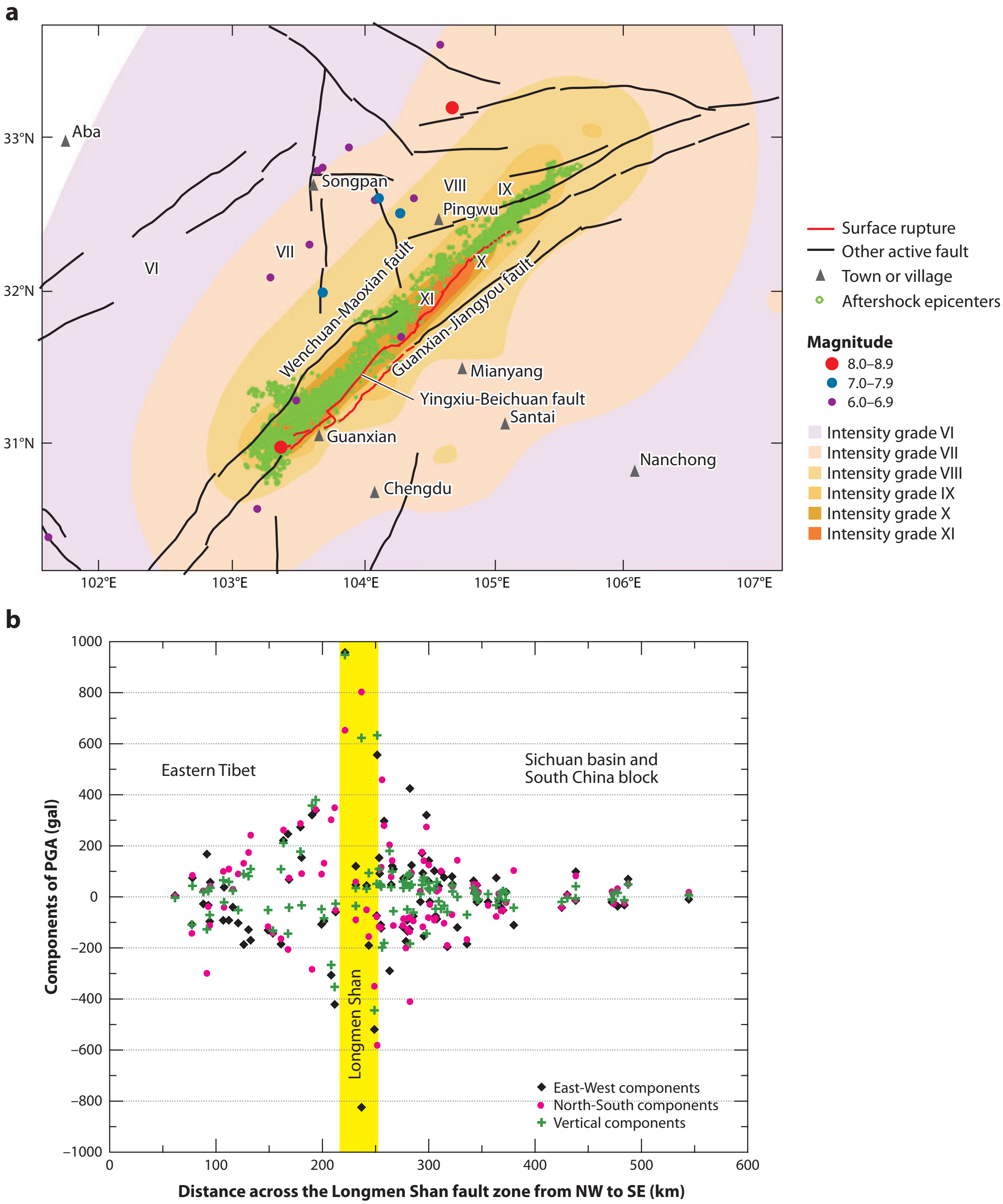

a
Aba
Songpan
Pingwu
Mianyang
Santai
Guanxian
Chengdu
Nanchong
VI
VII
VIII
IX
X
XI
Wenchuan-Maoxian fault
Guanxian-Jiangyou fault
Yingxiu-Beichuan fault
33°N
32°N
31°N
102°E
103°E
104°E
105°E
106°E
107°E
Surface rupture
Other active fault
Town or village
Aftershock epicenters
Magnitude
8.0–8.9
7.0–7.9
6.0–6.9
Intensity grade VI
Intensity grade VII
Intensity grade VIII
Intensity grade IX
Intensity grade X
Intensity grade XI
b
Eastern Tibet
Sichuan basin and
South China block
Longmen Shan
Components of PGA (gal)
Distance across the Longmen Shan fault zone from NW to SE (km)
East-West components
North-South components
Vertical components
1000
800
600
400
200
0
−200
−400
−600
−800
−1000
0
100
200
300
400
500
600

SUMMARY POINTS

1. Post-earthquake geological, seismological, and geodetic investigations all point to a cascading rupture of four segments, each of which has different geometry and behavior. The geometric complexity indicates structural discontinuities or barriers along the seismogenic fault that require complex rupture processes to overcome them.
2. Significant coseismic slip associated with the mainshock may occur in the shallow crust above 10-km depth, as corroborated by the aftershock hypocenter distribution and geodetic inversion for slip. This shallow slip then contributes to significant ground shaking.
3. The structure responsible for the Wenchuan earthquake is an imbricate, oblique, high-angle, listric, reverse fault that dips ∼70° above 15-km depth, then dips 30 to 40° below ∼15-km depth, and finally roots into the subhorizontal brittle-ductile transition zone below a depth of 20 to 22 km. Although many believe that dip-slip faults become listric at depth and root into a ductile lower crust, the Wenchuan earthquake rupture offers perhaps the clearest demonstration that such a listric structure exists.
4. Unlike an earthquake resulting from strain accumulation along a single fault, the Wenchuan earthquake involved three geological units: eastern Tibet, the Longmen Shan, and the Sichuan basin. Interactions among them caused slow strain accumulation in the Longmen Shan so that measurable preearthquake slip was minor. Coseismic deformation, however, took place mostly within the interseismically locked Longmen Shan fault zone. The earthquake may have initiated from slip on a fault plane dipping 30–40° northwest in a depth range of 15 to 20 km beneath the southwestern segment of the rupture zone and may have triggered oblique slip on the high-angle faults at depths shallower than 15 km to produce the great Wenchuan earthquake.

FUTURE ISSUES

1. Although we have inferred the seismogenic structure of the Longmen Shan fault to be an imbricate, high-angle, listric-reverse fault system, direct evidence is still needed through high-resolution, deep-seismic-sounding profiling.
2. Post-earthquake deformation will provide important information on the physical properties of both eastern Tibet's lithosphere, and especially its lower crust, and the Longmen Shan fault zone. Continuous GPS stations have been deployed after the earthquake. Analysis of postearthquake relaxation should reveal valuable information on the behavior of the lower crust in general.
3. Up to now, strain processes associated with the Wenchuan earthquake have been given in a qualitative, descriptive manner. To fully understand the interseismic, coseismic, and postearthquake processes, quantitative experiments of the various relevant processes are needed.

DISCLOSURE STATEMENT

The authors are not aware of any affiliations, memberships, funding, or financial holdings that might be perceived as affecting the objectivity of this review.

ACKNOWLEDGMENTS

This work has been a joint effort by many scientists who participated in emergency recovery and comprehensive studies after the Wenchuan earthquake. We thank all participants for their valuable contributions. We are grateful to the Sichuan Seismological Bureau for logistic support during the postearthquake comprehensive studies. Thanks also go to Li Ming and Tian Liu from the China Seismological Administration and Wang Li, Qi Guili, and Deng Yiwei from the Sichuan Seismological Bureau for their excellent administrative and logistical work that assured success of the comprehensive postearthquake studies. We thank Peter Molnar, Leigh Royden, Clark Burchfiel, Rob van der Hilst, and Eric Kirby for comments and encouragement. The work is supported by funds from the National Key Basic Research Program of China (2004CB418400), the State Key Laboratory of Earthquake Dynamics (LED2008A01), the China Earthquake Administration, and the National Science Foundation of China (40841013).

LITERATURE CITED

Ammon CJ, Ji C, Thio H-K, Robinson D, Ni S, et al. 2005. Rupture process of the 2004 Sumatra-Andaman earthquake. *Science* 308:1133–39

Avouac JP. 2003. Mountain building, erosion, and the seismic cycle in the Nepal Himalaya. *Adv. Geophys.* Vol. 46. 80 pp.

Bilham R, Gaur VK, Molnar P. 2001. Himalayan seismic hazard. *Science* 293:1442–44

Bollinger L, Avouac JP, Cattin T, Pandey MR. 2004. Stress buildup in the Himalaya. *J. Geophys. Res.* 109:B11405

Burchfiel BC, Chen Z, Liu Y, Royden LH. 1995. Tectonics of the Longmen Shan and adjacent regions, Central China. *Int. Geol. Rev.* 37:661–735

Burchfiel BC, Royden LH, van der Hilst RD, Hager BH, Chen Z, et al. 2008. A geological and geophysical context for the Wenchuan earthquake of 12 May 2008, Sichuan, People's Republic of China. *GSA Today* 18(7):4–11

Carena S, Suppe J, Kao H. 2002. The active detachment of Taiwan illuminated by small earthquakes and its control of first-order topography. *Geology* 30:935–38

CENC (China Earthquake Networks Center). 2008. **http://www.csi.ac.cn/sichuan/index080512001.htm**

Chang C-H, Wu Y-M, Zhao L, Wu T-T. 2007. Aftershocks of the 1999 Chi-Chi, Taiwan, earthquake: the first hour. *Bull. Seismol. Soc. Am.* 97:1245–58

Chen J, Liu Q, Li S, Guo B, Li Y, et al. 2009. Seismotectonics study by relocation of the Wenchuan Ms8.0 Earthquake sequence. *Chin. J. Geophys.* 52:390–97 (In Chinese with an English abstract)

Chen SF, Wilson CJL. 1996. Emplacement of the Longmen Shan Thrust-Nappe Belt along the eastern margin of the Tibetan Plateau. *J. Struct. Geol.* 18:413–30

Chen Z, Burchfiel BC, Liu Y, King RW, Royden LH, et al. 2000. Global Positioning System measurements from eastern Tibet and their implications for India/Eurasia intercontinental deformation. *J. Geophys. Res.* 105:16215–27

Chen Zh, Jia D, Zhang Q, Wei G, Li B, et al. 2005. Balanced cross-section analysis of the fold-thrust belt of the Longmen mountains. *Acta Geol. Sinica* 16:404–12

Clark MK, Bush J, Royden LH. 2005. Dynamic topography produced by lower crustal flow against rheological strength heterogeneities bordering the Tibetan Plateau. *Geophys. J. Int.* 162:575–90

Clark MK, Royden LH. 2000. Topographic ooze: building the eastern margin of Tibet by lower crustal flow. *Geology* 28:703–6

Densmore AL, Ellis MA, Li Y, Zhou R, Hancock GS, Richardson N. 2007. Active tectonics of the Beichuan and Pengguan faults at the eastern margin of the Tibetan Plateau. *Tectonics* 26:TC4005

Dietz LD, Ellsworth WL. 1997. Aftershocks of the Loma Prieta earthquake and their tectonic implications. *U.S. Geol. Surv. Prof. Pap.* 150-D:5–48

Global Centroid-Moment-Tensor (CMT) Project, **http://www.globalcmt.org/**

Hartzell SH, Heaton TH. 1983. Inversion of strong ground motion and teleseismic waveform data for the fault rupture history of the 1979 Imperial Valley, California, earthquake. *Bull. Seismol. Soc. Am.* 73(6A):1553–83

Hatzfeld D, Karakostas V, Ziazia M, Selvaggi G, Leborgne S, et al. 1997. The Kozani-Grevena (Greece) earthquake of May 13, 1995 revisited from a detailed seismological study. *Bull. Seismol. Soc. Am.* 87:463–73

Hauksson E, Jones L, Hutton K. 2002. The 1999 Mw 7.1 Hector Mine, California, earthquake sequence: complex conjugate strike-slip faulting. *Bull. Seismol. Soc. Am.* 92:1154–70

Hauksson E, Shearer P. 2005. Southern California hypocenter relocation with waveform cross-correlation, part 1: results using the double-difference method. *Bull. Seismol. Soc. Am.* 95:896–903

Hubbard J, Shaw JH. 2009. Uplift of the Longmen Shan and Tibetan Plateau, and the 2008 Wenchuan ($M = 7.9$) earthquake. *Nature* 458:194–97

Gan W, Zhang P-Z, Shen Z-K, Niu Z, Wang M, et al. 2007. Present-day crustal motion within the Tibetan Plateau inferred from GPS measurements. *J. Geophys. Res.* 112:B08416

Ji C. 2008. *Preliminary result of the May 12, 2008 Mw 7.97 ShiChuan earthquake*. **http://www.geol.ucsb.edu/faculty/ji/big_earthquakes/2008/05/12/ShiChuan.html**

Jia D, Wei G, Chen Z, Li B, Zeng Q, et al. 2006. Longmen Shan fold-thrust belt and its relation to the western Sichuan Basin in central China: new insights from hydrocarbon exploration. *AAPG Bull.* 90:1425–47

Kanamori H, Anderson DL. 1975. Theoretical basis of some empirical relations in seismology. *Bull. Seismol. Soc. Am.* 65:1073–95

King RW, Shen F, Burchfiel BC, Royden LH, Wang E, et al. 1997. Geodetic measurement of crustal motion in southwest China. *Geology* 25:179–82

Kirby E, Reiners PW, Krol MA, Whipple KX, Hodges KV, et al. 2002. Late Cenozoic evolution of the eastern margin of the Tibetan Plateau: inferences from $^{40}Ar/^{39}Ar$ and (U-Th)/He thermochronology. *Tectonics* 21(1):1001

Kirby E, Whipple K, Harkins N. 2008. Topography reveals seismic hazard. *Nat. Geosci.* 1:485–87

Kumar S, Wesnousky SG, Rockwell TK, Briggs RW, Thakur VC, Jayangondaperumal R. 2006. Paleoseismic evidence of great surface rupture earthquakes along the Indian Himalaya. *J. Geophys. Res.* 111:B03304

Kumar S, Wesnousky SG, Rockwell TK, Ragona D, Thakur VC, et al. 2001. Earthquake recurrence and rupture dynamics of Himalayan frontal thrust, India. *Science* 294:2328–31

Lavé J, Avouac J-P. 2000. Active folding of fluvial terraces across the Siwaliks Hills, Himalayas of central Nepal. *J. Geophys. Res.* 105:5735–70

Lavé J, Yule D, Sapkota S, Basant K, Madden C, et al. 2005. Evidence for a great medieval earthquake (~1100 A.D.) in the Central Himalayas, Nepal. *Science* 307:1302–5

Lay T, Kanamori H, Ammon CJ, Nettles M, Ward SN, et al. 2005. The great Sumatra-Andaman earthquake of 26 December 2004. *Science* 308(5725):1127–33

Li Ch, Zhang PZ, Yin J, Min W. 2009. Late Quaternary left-lateral slip rate of the Haiyuan fault, northeastern margin of the Tibetan Plateau. *Tectonics* 28:TC5010

Li H, Fu X, Van Der Woerd J. 2008. Surface rupture associated with the Wenchuan earthquake and its oblique slip. *Acta Geol. Sinica* 82:1623–43

Li SL, Lai XL, Yao ZX, Yang Q. 2009. Study on fault zone structures of northern and southern portions of the main central fault generated by Ms = 8.0 Wenchuan earthquake using fault-zone trapped waves. *Acta Seismol. Sinica* In press

Li SL, Zhang XK, Fan JC. 2005. Study on rupture zone of the $M = 8.1$ Kunlun Mountain earthquake using fault-zone trapped waves. *Acta Seismol. Sinica.* 27:43–52

Li X, Zhou Z, Huang M, Wen R, Yu H, et al. 2008. Preliminary analysis of strong-motion recordings from the magnitude 8.0 Wenchuan, China, earthquake of 12 May 2008. *Seismol. Res. Lett.* 79:844–54

Li YG, Aki K, Admas D, Hasemi A, Lee WHK. 1994. Seismic guided waves trapped in the fault zone of the Landers, California, earthquake of 1992. *J. Geophys Res.* 99:11705–22

Li YG, Chen P, Cochran ES, Vidale JE, Burdette T. 2006. Seismic evidence for rock damage and healing on the San Andreas fault associated with the 2004 M 6.0 Parkfield Earthquake. *Bull. Seismol. Soc. Am.* 96:S349–63

Li YG, Leary PG. 1990. Fault zone trapped seismic waves. *Bull. Seismol. Soc. Am.* 80:1245–71

Li YG, Vidale JE, Day SM, Oglesby DD, and the SCEC Field Working Team. Study of the. 1999. *M* 7.1 Hector Mine, California, earthquake fault plane by trapped waves. 2002. *Bull. Seismol. Soc. Am.* 92:1318–32

Liu J, Zhang Zh, Wen L. 2008. The Ms 8.0 Wenchuan earthquake co-seismic rupture and its tectonic implications—an out-of-sequence thrusting event with slip partitioned on multiple faults. *Acta Geol. Sinica* 82:1707–22 (In Chinese with an English abstract)

Liu Q, Li Y, Chen J, Guo B, et al. 2009. Wenchuan Ms8.0 earthquake: Preliminary study of the S-wave velocity structure of the crust and upper mantle. *Chin. J. Geophys.* 52:309–319 (In Chinese with an English abstract)

McCaffrey R. 2009. The tectonic framework of the Sumatran subduction zone. *Annu. Rev. Earth Planet. Sci.* 37:345–66

Mendoza C, Hartzell SH. 1988. Aftershock patterns and mainshock faulting. *Bull. Seismol. Soc. Am.* 78:1438–49

Nishimura N, Yagi Y. 2008. *Rupture process for May 12, 2008 Sichuan earthquake (preliminary result)*. **http://www.geol.tsukuba.ac.jp/~nisimura/20080512/**

Ouyed M, Yielding G, Hatzfeld D, King GCP. 1983. An aftershock study of the El Asnam (Algeria) earthquake of 1980 October 10. *Geophys. J. R. Astron. Soc.* 73:605–39

Ran Y, Chen L, Chen G, Yin J, Chen J, et al. 2008. Primary analysis of in-situ recurrence of large earthquake along seismogenic fault of the Ms 8.0 Wenchuan Earthquake, China. *Seismol. Geol.* 30:630–43 (In Chinese with English abstract)

Ran Y, Shi X, Wang H, Chen L, Chen J, et al. 2010. The maximum vertical co-seismic displacement and the style of deformation associated with the 2008 Wenchuan earthquake. *Chin. Sci. Bull.* 54:In press (In Chinese)

Royden LH, Burchfiel BC, King RW, Wang E, Chen Z, et al. 1997. Surface deformation and lower crustal flow in eastern Tibet. *Science* 276:788–90

Royden L, Burchfiel BC, van der Hilst RD. 2008. The geological evolution of the Tibetan Plateau. *Science* 321:1054–58

Shan X, Qu C, Song X, Zhang G, Liu Y, et al. 2009. Coseismic surface deformation caused by the Wenchuan earthquake from InSAR data analysis. *Chin. J. Geophys.* 52:496–504 (In Chinese with an English abstract)

Shen ZK, Lu J, Wang M, Bürgmann R. 2005. Contemporary crustal deformation around the southeast borderland of the Tibetan Plateau. *J. Geophys. Res.* 110:B11409

Shen ZK, Sun J, Zhang PZ, Wan Y, Wang M, et al. 2009. Slip maxima at fault junctions and rupturing of barriers during the 2008 Wenchuan earthquake. *Nat. Geosci.* 2:718–24

Sibson RH. 1986. Earthquakes and rock deformation in crustal fault zones. *Annu. Rev. Earth Planet. Sci.* 14:149–75

Sibson RH. 1989. Earthquake faulting as a structural process. *J. Struct. Geol.* 11:1–14

Sieh K, Jones L, Hauksson E, Hudnut K, Eberhart-Phillips D, et al. 1993. Near-field investigations of the Landers earthquake sequence, April to July 1992. *Science* 260:171–76

Sun J, Liang F, Shen ZK, Xu X. 2008. InSAR deformation observation and preliminary analysis of the Ms 8.0 Wenchuan earthquake. *Seismol. Geol.* 30:489–95 (In Chinese with an English abstract)

Thurber C, Zhang H, Waldhauser F, Hardebeck J, Michael A, Eberhart-Phillips D. 2006. Three-dimensional compressional wavespeed model, earthquake relocations, and focal mechanisms for the Parkfield, California, region. *Bull. Seismol. Soc. Am.* 96:S38–49

Waldhauser F, Ellsworth WL. 2000. A double-difference earthquake location algorithm: method and application to the Northern Hayward Fault, California. *Bull. Seismol. Soc. Am.* 90:1353–68

Wang CY, Han WB, Wu JP, Lou H, Chan WW. 2007. Crustal structure beneath the eastern margin of the Tibetan plateau and its tectonic implications. *J Geophys. Res.* 112:B07307

Wang CY, Mooney WD, Ding ZF, Yang JS, Yao ZX, Lou H. 2009. Shallow seismic structure of Kunlun fault zone in northern Tibetan Plateau, China: implications for the 2001 Ms8.1 Kunlun earthquake. *Geophys. J. Int.* 177(3):978–1000

Wang E, Meng Q. 2008. Discussion on tectonic evolution of the Longmen Shan fault zone. *Sci. China Ser. D* 38:1221–33

Wang W, Zhao L, Li J, Yao Zh. 2008. Rupture process of the Ms 8.0 Wenchuan earthquake of Sichuan, China. *Chin. J. Geophys.* 51:1403–10 (In Chinese with an English abstract)

Working Group of the Crustal Motion Observation Network of China Project. 2008. Coseismic displacement field of the 2008 Ms 8.0 Wenchuan earthquake determined by GPS. *Sci. China Ser. D* 38:1195–206 (In Chinese)

Xu L, Rondenay S, Van Der Hilst RD. 2007. Structure of the crust beneath the southeastern Tibetan Plateau from teleseismic receiver functions. *Phys. Earth Planet. Inter.* 165:176–93

Xu X, Wen X, Ye J, Ma B, Chen J, et al. 2008. The Ms 8.0 Wenchuan earthquake surface ruptures and its seismogenic structure. *Seismol. Geol.* 30:597–629 (In Chinese with an English abstract)

Xu X, Wen X, Yu G, Chen G, Klinger Y, et al. 2009. Coseismic reverse- and oblique-slip surface faulting generated by the 2008 Mw 7.9 Wenchuan earthquake, China. *Geology* 37:515–18

Xu Z. 2009. *Wenchuan Fault Scientific Drilling Program (WFSD)*. **http://www.wfsd.org/**

Xu Z, Ji S, Li H, Hou L, Fu X, Cai Z. 2008. Uplift of the Longmen Shan range and the Wenchuan earthquake. *Episodes* 31:291–301

Yao H, Beghein C, van der Hilst RD. 2008. Surface-wave array tomography in SE Tibet from ambient seismic noise and two-station analysis, II. Crustal and upper-mantle structure. *Geophys. J. Int.* 173:205–19

Yeats RS, Sieh K, Allen CR. 1997. *The Geology of Earthquakes*. Oxford Univ. Press. 576 pp.

Zhang PZ, Molnar P, Burchfiel BC, Royden L, Zhang W, et al. 1988. Bounds on the Holocene slip rate along the Haiyuan fault, north-central China. *Quat. Res.* 30:151–64

Zhang PZ, Slemmons DB, Mao F. 1991. Geometric pattern, rupture termination, and fault segmentation of the Dixie Valley–Pleasant Valley active normal fault system. *J. Struct. Geol.* 12:165–76

Zhang PZ, Deng Q, Zhang G, Ma J, Gan W, et al. 2003. Active tectonic blocks and strong earthquakes in continental China. *Sci. China Ser. D* 33(Suppl.):13–24

Zhang PZ, Shen Z, Wang M, Gan W, Bürgmann R, et al. 2004. Continuous deformation of the Tibetan Plateau from Global Positioning System data. *Geology* 32:809–12

Zhang PZ, Xu XW, Wen XZ, Rang RK. 2008. Slip rates and recurrence intervals of the Longmen Shan active fault zone and tectonic implications for the mechanism of the May 12 Wenchuan earthquake, 2008, Sichuan, China. *Chin. J. Geophys.* 51:1066–73 (In Chinese with an English abstract)

Zhang PZ. 2008. Tectonic deformation, strain partitioning, and crustal dynamics of the western Sichuan region. *Sci. China Ser. D* 38:1041–56 (In Chinese)

Zhang PZ, Wen X, Xu X, Gan W, Wang M, et al. 2009. Model of strain accumulation and release associated with the 2008 Wenchuan, Sichuan, China earthquake. *Chin. Sci. Bull.* 54:944–53 (In Chinese)

Zhang Y, Feng WP, Xu LS, Zhou CH, Chen YT. 2008. Spatio-temporal rupture process of the 2008 great Wenchuan earthquake. *Sci. China Ser. D* 52:145–154

Zhang Y, Xu L, Chen Y. 2009. Spatial-temporal variation of the source mechanism of the 2008 great Wenchuan earthquake. *Chin. J. Geophys.* 52:379–89

Zheng Y, Ma H, Lü J, Ni S, Li Y, Wei S. 2009. Source mechanism of strong aftershocks (Ms $\geq$ 5.6) of the 2008/05/12 Wenchuan earthquake and the implication for seismotectonics. *Sci. China Ser. D* 52(6):739–53

Zhou R, Li Y, Densmore AL, Ellis MA, He Y, et al. 2007. Active tectonics of the Longmen Shan region of the eastern margin of the Tibetan plateau. *Acta Geol. Sinica* 81:593–604

Zhu J. 2008. Background of the Wenchuan earthquake occurrence in deep structure and lithospheric dynamics. *J. Chengdu Univ. Technol.* 35:348–56 (In Chinese with an English abstract)